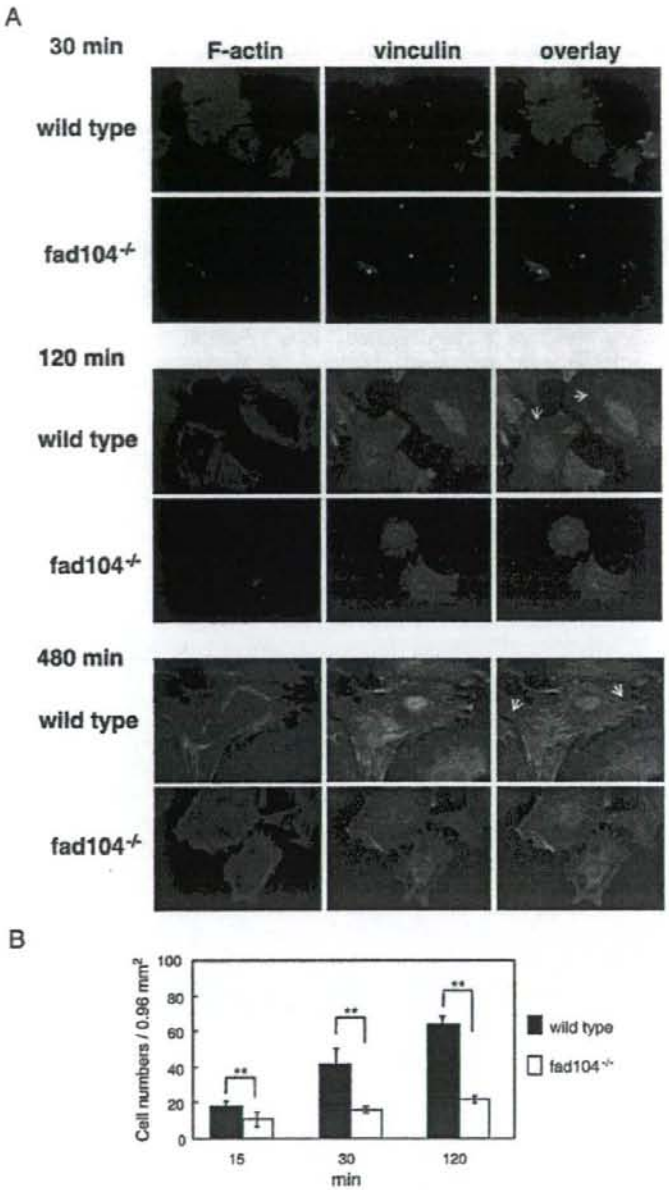

Fig. 7 – Deletion of *fad104* causes delayed stress fiber formation, cell adhesion and cell spreading. (A) Immunofluorescence of wild-type and *fad104*$^{-/-}$ MEFs. MEFs (4×10^4) from wild-type and *fad104*$^{-/-}$ embryos were plated on fibronectin-coated (3 μg/ml) cell disks in 24-well plates. At 30, 120 and 480 min from seeding, F-actin and vinculin were visualized with TRITC-conjugated phalloidin (red) and anti-vinculin antibody (green), respectively. Overlay demonstrates that the end of stress fibers co-localizes with vinculin (yellow). The arrow shows the typical end of stress fibers. A representative field at each time point is shown. (B) Cell adhesion assay of wild-type and *fad104*$^{-/-}$ MEFs. MEFs (1×10^4) from wild-type and *fad104*$^{-/-}$ embryos were plated onto fibronectin-coated (3 μg/ml) 24-well plates. At each time point, the attached cells were photographed, and counted in five random microscopic fields per plate. The data represent means with standard deviations ($n=5$). $^{**}p<0.01$.

were photographed and counted at 15, 30 and 120 min after plating. At all time points, the *fad104*$^{-/-}$ MEFs dramatically showed impaired adhesion compared with the wild-type MEFs (Fig. 7B). The results in Figs. 7A and B strongly suggest that *fad104* is a novel factor involved in cell adhesion and spreading.

Disruption of fad104 inhibited cell migration

Finally, we examined the effects of disruption of *fad104* on cell migration. The ability of cells to migrate was evaluated with a wound healing assay. The confluent monolayers of wild-type and *fad104*$^{-/-}$ MEFs were wounded with a yellow tip. The damaged area was photographed and measured at the time of wounding. The wound of wild-type MEFs gradually healed and was almost closed after 10 h. On the other hand, wound closure for *fad104*$^{-/-}$ MEFs was remarkably delayed, and the wound was not completely closed within 10 h (Fig. 8A). The area of the wound that was not covered by migrating cells within 10 h was measured by NIH-Image J software (Fig. 8B). At all time points, the wound closure of *fad104*$^{-/-}$ MEFs was notably and significantly repressed compared to that of wild-type MEFs. Even after 10 h, almost half the area was still uncovered in *fad104*$^{-/-}$ MEFs. These results indicate that *fad104* is necessary for cell migration.

Discussion

The molecular mechanism of adipocyte differentiation is very complex. Previous studies indicated that transcription factors including PPARγ, the C/EBP family and SREBP-1 regulated the differentiation process. MEFs prepared from PPARγ-deficient mice failed to differentiate into adipocytes [25]. Furthermore, the double knockout of C/EBPβ and C/EBPδ impaired the synthesis of fat in mice [24]. SREBP-1 is known to be required for production of ligands of PPARγ [26]. However, these three families of transcription factors are expressed at the middle and late stages of adipogenesis. On the other hand, it is not clear which factors regulate adipocyte differentiation at the initial stage.

Previously, we identified many genes that were expressed early on in the differentiation of 3T3-L1 cells into adipocytes [4,5]. *fad104* is a novel gene included among the isolated genes. Since knockdown of its expression inhibited the differentiation process, *fad104* has indispensable roles in the differentiation of 3T3-L1 preadipocytes. However, little was known about the functions and physiological roles of *fad104*.

In this study, to examine the actual biological functions of *fad104*, we generated mice with a homozygous null *fad104*

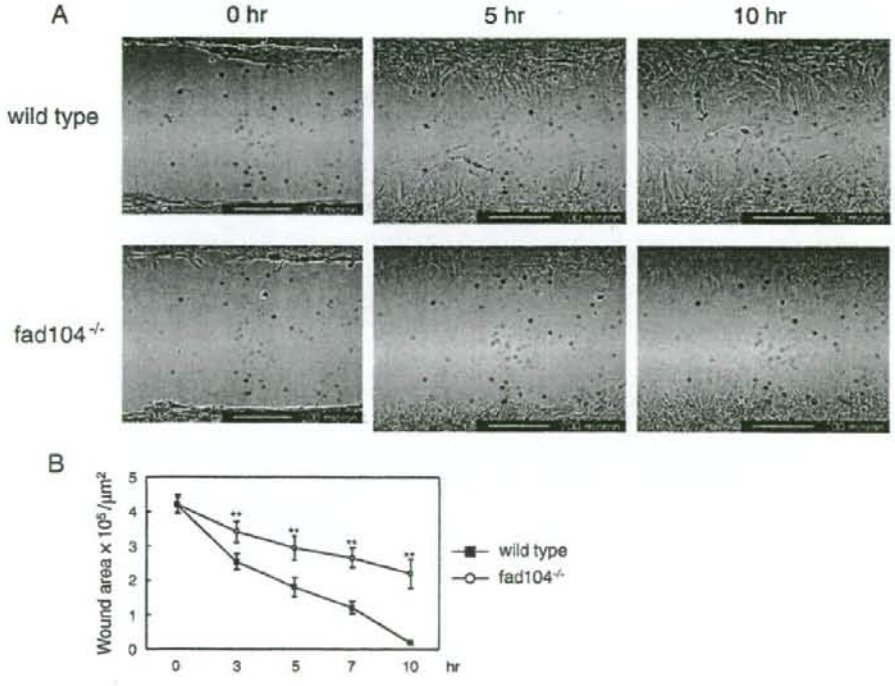

Fig. 8 – Disruption of *fad104* inhibits cell migration in wound healing assay. (A) Wound healing assay of wild-type (top panels) and *fad104*$^{-/-}$ MEFs (bottom panels). MEFs were plated and grown to confluence. At 1 day postconfluence, a wound was introduced into the monolayer, and the migration of cells was monitored using photographs taken at time points from 0 to 10 h. The 0, 5 and 10 h time points are shown for each cell line. (B) Quantification of the wound healing assay shown in panel A. For each cell line, the wound area was quantified by using NIH-Image J software. The data represent means with standard deviations ($n=4$). $^{**}p<0.01$.

mutation. Interestingly, the *fad104*-deficient mice died within 1 day of birth. All of the *fad104*-deficient pups at E18.5 were breathing and moving just after caesarean section, suggesting that the disruption of *fad104* caused rapid postnatal death. It is well known that the maintenance of blood glucose levels and the thermoregulation have pivotal roles for survival of newborn pups just after birth [27,28]. However, as shown Fig. 2, *fad104*-deficient neonates did not exhibit the abnormalities about blood glucose level, body temperature, and BAT weight. In our previous reports, *fad104* was found to be highly expressed in white adipose tissue (WAT). On the other hand, *fad104* was also modestly expressed in heart, kidney and lung [12]. Since little WAT is found in newborns, it is possible that the postnatal lethality observed in *fad104*-deficient mice is caused by a functional disorder of *fad104* in organs including the heart, kidney and lung. In order to elucidate the cause of the rapid death after birth of *fad104*-deficient mice, a pathological analysis of these organs is now ongoing.

Kuma et al. indicated that mice deficient for *Atg5*, which is essential for autophagosome formation, die within 1 day at birth, suggesting that autophagic degradation of proteins is important for survival during neonatal starvation [29]. We attempted to examine whether *fad104* is involved in the regulation of autophagic activity. During autophagy, microtubule-associated protein light chain (LC3) is processed from the cytosolic form, LC3-I, to the membrane-bound form, LC3-II. Since the amount of LC3-II correlates with the number of autophagosomes, immnoblotting of endogenous LC3 can be used to measure autophagic activity. Therefore, we performed Western blotting analysis using the cell lysates prepared from wild-type and *fad104*$^{-/-}$ MEFs under nutrition starvation. Commercially available anti-LC3 antibody, which was employed the detection of endogenous LC3 in MEFs was used [30]. However, we could detect neither LC3-I nor LC3-II in the cell lysates prepared from wild-type and *fad104*$^{-/-}$ MEFs, whereas both LC3-I and LC3-II proteins were detected in the cell lysate prepared from HeLa cells under starvation condition as described previously [31]. Although we could not conclude whether *fad104* is related to autophagic activity in this study, it is necessary to elucidate the relationship between *fad104* and autophagic activity by further analyses.

Although it is well known that the proteins containing the fibronectin type III domain localize to the cell surface, the FAD104 localized to the ER, but not the plasma membrane. Therefore, FAD104 may be a novel protein localized to the ER. The proteins found in the ER have an important role of various cellular functions. For example, calreticulin, a Ca^{2+}-binding protein of the ER, influences the cell spread and cell adhesion via the regulation of c-Src activities and vinculin expression [32,33]. Therefore, we next examined whether a novel gene, *fad104*, also is involved in various cellular functions. Analyses of MEFs prepared from *fad104*-deficient mice demonstrated *fad104* to be crucial for cell proliferation, adhesion, spreading and migration.

As shown in Fig. 6, the disruption of *fad104* caused the reduction of the increase of the cell numbers during 6 days after seeding. This result indicates that the proliferation rate of *fad104*$^{-/-}$ MEFs was slightly attenuated than that of wild-type MEFs. *Fad104*-deficient MEFs also exhibited a delay in cell adhesion and cell spreading (Fig. 7). It is necessary to explore the mechanism which *fad104* regulates the cell proliferation.

Cell migration, cell spreading and adhesive properties are regulated by continuous remodeling of the actin cytoskeleton. For example, in cell migration, the actin structures are divided into three steps: the lamelipodial actin network at the leading edge of the cell, filopodial bundles beneath the plasma membrane, and contractile actin stress fibers in the cytoplasm [34]. At the early stage of adipocyte differentiation, the change to the actin organization is very important. Kawaguchi et al. indicated that ADAM12, a disintegrin and metalloprotease, altered the organization of the actin cytoskeleton and extracellular matrix by impairing the function of β1 integrin, and induced differentiation into mature adipocytes [35]. A deficiency of *fad104* dramatically reduces the formation of stress fibers, strongly suggesting that *fad104* also functions as a key regulator of the actin cytoskeleton's organization, and may promote adipogenesis in the early stages of the differentiation process.

Recently, Obholz et al. reported that a fibronectin type III domain containing 3a (FNDC3A) is necessary for adhesion between spermatids and Sertoli cells, and the mutation of *fndc3a* is the cause of male sterility in symplastic spermatids (sys) mice [36]. FNDC3a is closely related to FAD104, since FNDC3a also contains 9 repeats of the fibronectin type III domain and transmembrane domain. It is of interest that FNDC3a is also necessary for mediating adhesion during spermatogenesis. However, FNDC3a does not have a RGD tripeptide sequence in any fibronectin type III domain repeat sequence. In addition, the disruption of FNDC3a does not cause postnatal death. Thus, although FAD104 and FNDC3a are very similar, these two proteins might have distinct and different roles in cellular functions and developmental processes.

In summary, the present study provided some new insights into the functions of a novel gene, *fad104*, namely as essential for the survival of newborns just after birth and as important for cell proliferation, adhesion, spreading and migration. Although further investigation is definitely needed, *fad104* may play an important role in the late stage of embryonic development or neonates after birth via the regulation of cell proliferation, adhesion, spreading and migration. Furthermore, it is possible that *fad104* regulates these cellular functions by altering the actin cytoskeleton's organization. Although we have no information on how *fad104* regulates the survival of neonates or adipocyte differentiation yet, further analyses of *fad104* would help us to understand not only the signaling pathways at the early stage of adipocyte differentiation but also the molecular mechanisms of survival after birth.

Acknowledgments

We thank Dr. Kei Tominaga and Chiharu Kondo for the construction of targeting vectors and screening of positive ES clones. We are grateful to Misaki Fujimura for the construction of fad104 expression plasmid. We also thank Dr. Takashi Ueda for histological analyses. This work was supported in part by grants from the Ministry of Education, Culture, Sports, Science and Technology (MEXT), Japan, Japan Society for the Promotion of Science (JSPS), the grant-in-aid for research in Nagoya City University, and the Takeda Science Foundation.

REFERENCES

[1] P.G. Kopelman, Obesity as a medical problem, Nature 404 (2000) 635–643.
[2] R.P. Brun, J.B. Kim, E. Hu, S. Altiok, B.M. Spiegelman, Adipocyte differentiation: a transcriptional regulatory cascade, Curr. Opin. Cell Biol. 8 (1996) 826–832.

[3] E.D. Rosen, C.J. Walkey, P. Puigserver, B.M. Spiegelman, Transcriptional regulation of adipogenesis, Genes Dev. 14 (2000) 1293–1307.
[4] M. Imagawa, T. Tsuchiya, T. Nishihara, Identification of inducible genes at the early stage of adipocyte differentiation of 3T3-L1 cells, Biochem. Biophys. Res. Commun. 254 (1999) 299–305.
[5] M. Nishizuka, T. Tsuchiya, T. Nishihara, M. Imagawa, Induction of Bach1 and ARA70 gene expression at an early stage of adipocyte differentiation of mouse 3T3-L1 cells, Biochem. J. 361 (2002) 629–633.
[6] M. Nishizuka, K. Honda, T. Tsuchiya, T. Nishihara, M. Imagawa, RGS2 promotes adipocyte differentiation in the presence of ligand for peroxisome proliferator-activated receptor gamma, J. Biol. Chem. 276 (2001) 29625–29627.
[7] M. Nishizuka, E. Arimoto, T. Tsuchiya, T. Nishihara, M. Imagawa, Crucial role of TCL/TC10beta L, a subfamily of Rho GTPase, in adipocyte differentiation, J. Biol. Chem. 278 (2003) 15279–15284.
[8] A. Kitamura, M. Nishizuka, K. Tominaga, T. Tsuchiya, T. Nishihara, M. Imagawa, Expression of p68 RNA helicase is closely related to the early stage of adipocyte differentiation of mouse 3T3-L1 cells, Biochem. Biophys. Res. Commun. 287 (2001) 435–439.
[9] K. Tominaga, Y. Johmura, M. Nishizuka, M. Imagawa, Fad24, a mammalian homolog of Noc3p, is a positive regulator in adipocyte differentiation, J. Cell. Sci. 117 (2004) 6217–6226.
[10] K. Tominaga, T. Kagata, Y. Johmura, T. Hishida, M. Nishizuka, M. Imagawa, SLC39A14, a LZT protein, is induced in adipogenesis and transports zinc, FEBS J. 272 (2005) 1590–1599.
[11] K. Tominaga, C. Kondo, T. Kagata, T. Hishida, M. Nishizuka, M. Imagawa, The novel gene fad158, having a transmembrane domain and leucine-rich repeat, stimulates adipocyte differentiation, J. Biol. Chem. 279 (2004) 34840–34848.
[12] K. Tominaga, C. Kondo, Y. Johmura, M. Nishizuka, M. Imagawa, The novel gene fad104, containing a fibronectin type III domain, has a significant role in adipogenesis, FEBS Lett. 577 (2004) 49–54.
[13] Y. Johmura, S. Osada, M. Nishizuka, M. Imagawa, FAD24 acts in concert with histone acetyltransferase HBO1 to promote adipogenesis by controlling DNA replication, J. Biol. Chem. 283 (2008) 2265–2274.
[14] D. Craig, M. Gao, K. Schulten, V. Vogel, Structural insights into how the MIDAS ion stabilizes integrin binding to an RGD peptide under force, Structure 12 (2004) 21–30.
[15] R. Pankov, K.M. Yamada, Fibronectin at a glance, J. Cell. Sci. 115 (2002) 3861–3863.
[16] S.K. Sastry, K. Burridge, Focal adhesions: a nexus for intracellular signaling and cytoskeletal dynamics, Exp. Cell Res. 262 (2000) 25–36.
[17] B.H. Geiger, A. Bershadsky, R. Pankov, K.M. Yamada, Transmembrane crosstalk between the extracellular matrix–cytoskeleton crosstalk, Nat. Rev. Mol. Cell Biol. 2 (2002) 793–805.
[18] R.D. Bowditch, M. Hariharan, E.F. Tominna, J.W. Smith, K.M. Yamada, E.D. Getzoff, M.H. Ginsberg, Identification of a novel integrin binding site in fibronectin. Differential utilization by beta 3 integrins, J. Biol. Chem. 269 (1994) 10856–10863.
[19] T. Nagai, N. Yamakawa, S. Aota, S.S. Yamada, S.K. Akiyama, K. Olden, K.M. Yamada, Monoclonal antibody characterization of two distant sites required for function of the central cell-binding domain of fibronectin in cell adhesion, cell migration, and matrix assembly, J. Cell Biol. 114 (1991) 1295–1305.
[20] B.M. Spiegelman, S.D. Farmer, Decreases in tubulin and actin gene expression prior to morphological differentiation of 3T3 adipocytes, Cell 29 (1982) 53–60.
[21] B.M. Spiegelman, C.A. Ginty, Fibronectin modulation of cell shape and lipogenic gene expression in 3T3-adipocytes, Cell 35 (1983) 657–666.
[22] L. Yang, L. Wang, Y. Zheng, Gene targeting of Cdc42 and Cdc42GAP affirms the critical involvement of Cdc42 in filopodia induction, directed migration, and proliferation in primary mouse embryonic fibroblasts, Mol. Biol. Cell 17 (2006) 4675–4685.
[23] F. Chen, Y. Lu, V. Castranova, Z. Li, M. Karin, Loss of IKKβ promotes migration and proliferation of mouse embryo fibroblast cells, J. Biol. Chem. 281 (2006) 37142–37149.
[24] T. Tanaka, N. Yoshida, T. Kishimoto, S. Akira, Defective adipocyte differentiation in mice lacking the C/EBPbeta and/or C/EBPdelta gene, EMBO J. 16 (1997) 7432–7443.
[25] N. Kubota, Y. Terauchi, H. Miki, H. Tamemoto, T. Yamauchi, K. Komeda, S. Satoh, R. Nakano, C. Ishii, T. Sugiyama, K. Eto, Y. Tsubamoto, A. Okuno, K. Murakami, H. Sekihara, G. Hasegawa, M. Naito, Y. Toyoshima, S. Tanaka, K. Shiota, T. Kitamura, T. Fujita, O. Ezaki, S. Aizawa, R. Nagai, K. Tobe, S. Kimura, T. Kadowaki, PPAR gamma mediates high-fat diet-induced adipocyte hypertrophy and insulin resistance, Mol. Cell 4 (1999) 597–609.
[26] J.B. Kim, B.M. Spiegelman, ADD1/SREBP1 promotes adipocyte differentiation and gene expression linked to fatty acid metabolism, Genes Dev. 10 (1996) 1096–1107.
[27] B. Cannon, J. Nedergaard, Brown adipose tissue: function and physiological significance, Physiol. Rev. 84 (2004) 277–359.
[28] M.E. Symonds, M.A. Lomax, Material and environmental influences on thermoregulation in the neonate, Proc. Nutr. Soc. 51 (1992) 165–172.
[29] A. Kuma, M. Hatano, M. Matsui, A. Yamamoto, H. Nakaya, T. Yoshimori, Y. Ohsumi, T. Tokuhisa, N. Mizushima, The role of autophagy during the early neonatal starvation period, Nature 432 (2004) 1032–1035.
[30] C.P. Cheng, M.C. Yang, H.S. Liu, Y.S. Lin, H.Y. Lei, Concanavalin A induces autophagy in hepatoma cells and has a therapeutic effect in a murine in situ hepatoma model, Hepatology 45 (2007) 286–296.
[31] Y. Kabeya, N. Mizushima, T. Ueno, A. Yamamoto, T. Kirisako, T. Noda, E. Kominami, Y. Ohsumi, T. Yoshimori, LC3, a mammalian homologue of yeast Apg8p, is localized in autophagosome membranes after processing, EMBO J. 19 (2000) 5720–5728.
[32] S. Papp, M.P. Fadel, H. Kim, C.A. McCulloch, M. Opas, Calreticulin affects fibronectin-based cell-substratum adhesion via the regulation of c-Src activity, J. Biol. Chem. 282 (2007) 16585–16598.
[33] M. Opas, M.S. Pawlikowski, G.K. Jass, N. Mesaeli, M. Michalak, Calreticulin modulates cell adhesiveness via regulation of vinculin expression, J. Cell Biol. 135 (1996) 1913–1923.
[34] P. Hatulainen, P. Lappalainen, Stress fibers are generated by two distinct actin assembly mechanisms in motile cells, J. Cell Biol. 173 (2006) 383–394.
[35] N. Kawaguchi, C. Sundberg, M. Kveiborg, B. Moghadaszadeh, M. Asmar, N. Dietrich, C.K. Thodeti, F.C. Nielson, P. Moller, A.M. Mercurio, R. Albrechtsen, U.M. Wewer, ADAM12 induces actin cytoskeleton and extracellular matrix reorganization during early adipocyte differentiation by regulating beta1 integrin function, J. Cell. Sci. 116 (2003) 3893–3904.
[36] K.L. Obholz, A. Akopyan, K.G. Waymire, G.R. MacGregor, FNDC3A is required for adhesion between spermatids and Sertoli cells, Dev. Biol. 298 (2006) 498–513.

Biochemical and Biophysical Research Communications 380 (2009) 460–466

Contents lists available at ScienceDirect

Biochemical and Biophysical Research Communications

journal homepage: www.elsevier.com/locate/ybbrc

Ptpcd-1 is a novel cell cycle related phosphatase that regulates centriole duplication and cytokinesis

Doaa H. Zineldeen, Midori Shimada, Hiroyuki Niida, Yuko Katsuno, Makoto Nakanishi *

Department of Cell Biology and Biochemistry, Graduate School of Medical Sciences, Nagoya City University, 1 Kawasumi, Mizuho-cho, Mizuho-ku, Nagoya 467-8601, Japan

ARTICLE INFO

Article history:
Received 6 January 2009
Available online 24 January 2009

Keywords:
Centrosome
Phosphatase
Mitosis
Polo-like kinases
Cytokinesis
Cdc14

ABSTRACT

Proper progression of mitosis requires spatio-temporal regulation of protein phosphorylation by orchestrated activities of kinases and phosphatases. Although many kinases, such as Aurora kinases, polo-like kinases (Plks), and cyclin B-Cdk1 are relatively well characterized in the context of their physiological functions at mitosis and regulation of their enzymatic activities during mitotic progression, phosphatases involved are largely unknown. Here we identified a novel protein tyrosine phosphatase containing domain 1 (Ptpcd 1) as a mitotic phosphatase, which shares sequence homology to Cdc14. Immunofluorescence studies revealed that Ptpcd1 partially colocalized with γ-tubulin, an archetypical centrosomal marker. Overexpression of this phosphatase prevented unscheduled centrosomal amplification in hydroxyurea arrested U2OS cells. Intriguingly, Ptpcd 1-associated and colocalized with polo-like kinase 1(Plk1). Hence, overexpression of Ptpcd1 rescued prometaphase arrest of Plk-1 depleted cells, but resulted in aberrant cytokinesis as did as Plk1 overexpression. These results suggested that Ptpcd1 is involved in centrosomal duplication and cytokinesis.

© 2009 Elsevier Inc. All rights reserved.

Faithful transmission of genetic information relies on the coordinated regulatory system of the cell cycle [1]. In higher eukaryotes, mitosis involves many dynamic processes at chromosomes, including condensation and segregation, both of which are mainly regulated by protein phosphorylation and dephosphorylation [2]. Proper segregation of chromosomes requires centrosomal maturation, separation, spindle formation and alignment of chromosomes [2,3]. Centrosome is the major microtubule organizing center in animal cells composed of two centrioles, which are barrel shaped structures with nine triple microtubules and a pericentriolar matrix responsible for nucleating microtubules and organizing mitotic spindles for bipolar separation of sister chromatids [4,5]. The identification of several centrosome-associated protein kinases has proposed the concept that multiple regulatory phosphorylation pathways tightly control centrosome cycle during cell cycle [6–8]. Around G1/S transition, a procentriole forms adjacent to each parental centriole and continues growing during S phase. At the onset of mitosis, the two centrosomes separate and the daughter centriole matures and instructs mitotic spindle formation [4]. In post-mitotic cells, centrosome migrates to the cell surface and one of the centrioles differentiates into a basal body that nucleates microtubules to form a cilium [5].

Polo-like kinases (Plks) regulate a multitude of several mitotic processes, including centrosome duplication, maturation [9], bipolar spindle formation [10], microtubule/kinetochore interactions, and cytokinesis [11,12]. Spatio-temporal coordination of Plks activities is achieved through binding to phosphorylated docking proteins with distinct subcellular localizations, such as centrosomes, kinetochore, and the midzone [12,13]. At early mitosis, Cdk1 creates the phosphorylated docking sites on the substrates [1], whereas Plks create their own docking sites on other partners after inactivation of Cdk1 [1,12,13]. In budding yeast, some parts of mitotic function of Plks appear to be mediated by Cdc14p. Cells lacking Cdc14p are unable to exit from mitosis, with defects in both movement of chromosomes to the spindle poles and elongation of anaphase spindles [14]. Mammalian cells possess two Cdc14 paralogue, Cdc14A and Cdc14B, identified based on their sequence similarity to Cdc14p [15]. Recent studies suggested that Cdc14A and Cdc14B might be involved in distinctive cellular functions; the former functioned in centrosomal separation and cytokinesis [3,16], and the latter in centrosomal duplication and microtubule stabilization [17]. However, Cdc14B deficient cells were viable and lacked apparent defects in chromosome segregation and cytokinesis [18], suggesting that alternative phosphatase(s) might be capable of complementing the mitotic functions of Cdc14B. Here, we identified Ptpcd1 as a possible functional isozyme of mammalian Cdc14B that is genetically linked to Plk1.

Materials and methods

Cloning of Ptpcd1. The complete ORF of Ptpcd1 (corresponding exactly to AW456874; No. NM 207232 and MGI: 2145430) was

* Corresponding author. Fax: +81 52 842 3955.
E-mail address: mkt-naka@med.nagoya-cu.ac.jp (M. Nakanishi).

0006-291X/$ - see front matter © 2009 Elsevier Inc. All rights reserved.
doi:10.1016/j.bbrc.2009.01.113

amplified by PCR using mouse brain cDNA library as a template with the following primer set: 5′-ATG GCG CAG GAG TCT TGC CA-3′ and 5′-TCA GGA GAG GCT GCT GTC CTT TTT GC-3′. The PCR product was subcloned into pCR II-TOPO (Invitrogen). pcDNA3.1-Myc/HisPtpcd1 was then generated by subcloning of the KpnI/NotI fragment into pcDNA3.1Myc/His vector. The KpnI/NotI fragment was amplified by PCR using pCRII-TOPOPtpcd1 as a template with a set of primers; 5′-TTT GAA TTC GCC ACC ATG TCG TCC GGG GCC AAG GAG-3′and 5′-AAA TCT AGA GGG CAG AGG GGT CCC GTT-3′. pcDNA3.1Plk1-HA was generated by subcloning of EcoRI/NotI fragment from pET23d-Plk1 (kind gift from Dr. Nishida) into pcDNA3.1HA.

Cell culture. HeLa and U2OS cells were cultured and maintained in Dulbecco's modified Eagle's medium (Invitrogen) supplemented with 10% fetal bovine serum as described previously [19]. Nocodazole and hydroxyurea were purchased from Sigma.

Knockdown experiments. Plasmid transfections were performed using FuGENE6 transfection reagent (Roch) according to manufacturer's instruction. Stealth siRNAs for Plk1 (Invitrogen) or control (Invitrogen) were transfected using lipofectamin 2000 (Invitrogen).

Immunoblotting. Antibodies used in this study were anti-c-myc (sc-789; Santa Cruz, sc-40; Santa Cruz), anti-pTyr-Cdk1 (9111; Cell signaling), anti-cyclin B1 (GNS1; Santa Cruz), anti-Plk1 (35-200; upstate), anti-HA (12CA5; Roch), anti-γ-tubulin (T3559; Sigma) and anti-α-tubulin (Sigma). Whole cell extracts were prepared as described previously [20] and were subjected to immunoblotting. For IP-immunoblotting, U2OS cells were cotransfected with Plk1-HA, along with Ptpcd1-myc or empty pcDNA3.1. Cells were harvested in RIPA buffer (10 mM Tris–HCl, pH7.5, 150 mM NaCl, 0.5% Triton X-100, 1% sodium deoxycholate and complete protease inhibitor tablets (1/10 ml) (Roch). The lysates (200 μg) were incubated with anti-myc antibodies (5 μg) or mouse normal IgG as a control at 4 °C for 1 h and then precipitated with 20 μl of protein G beads. The resultant precipitates were separated by SDS–PAGE and then analyzed by immunoblotting.

Microtubule regrowth assay. Cells on coverslips were treated with 4 mM nocodazole for 30 min at 37 °C, followed by replacement with normal medium. Cells were fixed at −20 °C with methanol and immunostained for immunofluorescence microscopy was performed as described previously [21].

Immunofluorescence analysis. Secondary antibodies for immunofluorescence microscopy were Cy3 (Jackson immunoresearch), Alexa 594 and Alexa 488 (Molecular probes). Cells on coverslips were fixed in 4% PFA for 10 min at RT and then permeabilized with 0.25% Triton X-100 in PBS. Blocking was done in 5% normal goat serum (Convac) containing 1% Triton X-100. Fixed cells were incubated with antibodies in blocking for 1 h at RT. DNA was counterstained with DAPI (2 mg/ml). For centrosomal staining, cells were fixed with methanol at −20 °C for 10 min.

Results and discussion

Ptpcd 1 is a centrosomal phosphatase that regulates centrosomal duplication during S phase

Immotile primary cilium is a centriole-based organelle that consists of microtubule pairs located at the plasma membrane [22]. The fact that a cilium is differentiated from centrosomes after mitosis has suggested that the function and structures of cilia are regulated by similar mechanisms to those of centrosomes [23]. Indeed, Nek2 and Aurora A kinases are involved in the regulation of both centrosomes and cilia functions [24]. Ptpcd 1 was originally identified as a dual specificity protein phosphatase highly expressed in mouse cilia [25]. We therefore speculated that Ptpcd 1 might be involved in the regulation of centrosomal function. Ptpcd 1 encodes a 721 amino acid protein with a predicated molecular weight of 82 kDa. Sequence analysis of Ptpcd1 revealed the significant homology with yeast Cdc14p with coiled coil domain at its carboxyl terminal, RXXL motif (a putative APC/C binding motif), several nuclear localization signals (Suppl. Fig. 1A), and a putative nuclear export signal (Suppl. Fig. 1B). To examine whether Ptpcd1 functions at centrosomes, Ptpcd1-myc was transfected into HeLa cells. In interphase cells, signals corresponding to Ptpcd1 were detected at both cytoplasm and nucleus with one or two closely spaced dots. Importantly, these dot signals were localized adjacent to, but not overlapped with, the signals from γ-tubulin, a centrosomal protein, raising the possibility of its centriolar localization (Fig. 1A). This centrosomal enrichment of Ptpcd1 was observed from interphase to anaphase, whereas it was hardly detected at telophase where most of the immunoreactivity was detected at midbody. This spatio-temporal localization in relation to cell cycle conveyed that Ptpcd1 might be a novel centrosomal-related phosphatase.

In certain transformed cells, such as U2OS cells, prolonged S phase arrest by hydroxyurea (HU) causes uncoupled centrosomal duplication from cell cycle with multiple rounds of centriole duplication in the absence of DNA replication and mitotic division (Fig. 1B, upper panel) [15]. In order to examine whether Ptpcd-1 plays a role in the regulation of centriole duplication, Ptpcd1 were overexpressed into U2OS cells in the presence of 4 mM HU for 72 h. Ptpcd 1 expression inhibited HU-induced centriole over duplication (Fig. 1B, lower panel). Majority of control U2OS cells possessed more than single centrosome when cells were treated with HU. In contrast, 60% of Ptpcd 1 expressing cells possessed single centrosome (Fig. 1C). These results clearly indicated that overexpression of Ptpcd1 suppressed uncoupled centrosomal duplication during S phase. Given that Cdk activity regulates centrosomal duplication during S phase, we asked whether Ptpcd1 affect inhibitory phosphorylation of Cdc2 at Y15, which is regulated at centrosomes during S to G2 phase. Cdc2 phosphorylation at Y15 slightly decreased, whereas expression of cyclin B1 was not affected by Ptpcd1 expression (Fig. 1D).

Ptpcd1 associates with Plk1 and is involved in the regulation of mitotic progression

Plk1 regulates centrosomal functions at multiple levels, such as centrosomal stabilization, nucleation, duplication, microtubule stabilization, and cytokinesis [9–13]. Therefore, Ptpcd1 might be involved in Plk1-dependent regulation of centrosome functions. To examine this possibility, we first asked whether Ptpcd1 physically interact with Plk1. Plk1-HA and Ptpcd1-myc were co-transfected into HeLa cells and the cell extracts were immunoprecipitated with anti-myc antibodies. Plk1-HA as well as Ptpcd1-myc was readily detected in the myc-immunoprecipitates, indicating that Plk1-HA was capable of forming a complex with Ptpcd1-myc (Fig. 2A). Immunocytochemical analysis revealed colocalization of ectopically expressed Ptpcd1-myc with endogenous Plk1 (Fig. 2B). Intriguingly, Ptpcd1-myc appeared to accumulate and colocalize with Plk1 at mid-body in telophase cells. These results suggested that Ptpcd1 might also function in cytokinesis as Plk1 did [1]. To address this question, we examined the effect of Ptpcd1 overexpression on mitotic progression. Aberrant cytokinesis in the form of fused or intercellular α-tubulin bridges was apparent in cells expressing Ptpcd1 (Fig. 3A and C). Hence, an increase in the number of cells with multiple nuclei was observed when Ptpcd1 was overexpressed (Fig. 3B and C). These results suggested that Ptpcd1 as well as Plk1 as reported played an important role in cytokinesis.

In addition to cytokinesis, Plk1 was reported to stabilize microtubule organization [10,12]. Therefore, we then asked if Ptpcd1 expression affect the microtubule stabilization. HeLa cells were transfected with pcDNA3.1Ptpcd1-myc and treated with nocodaz-

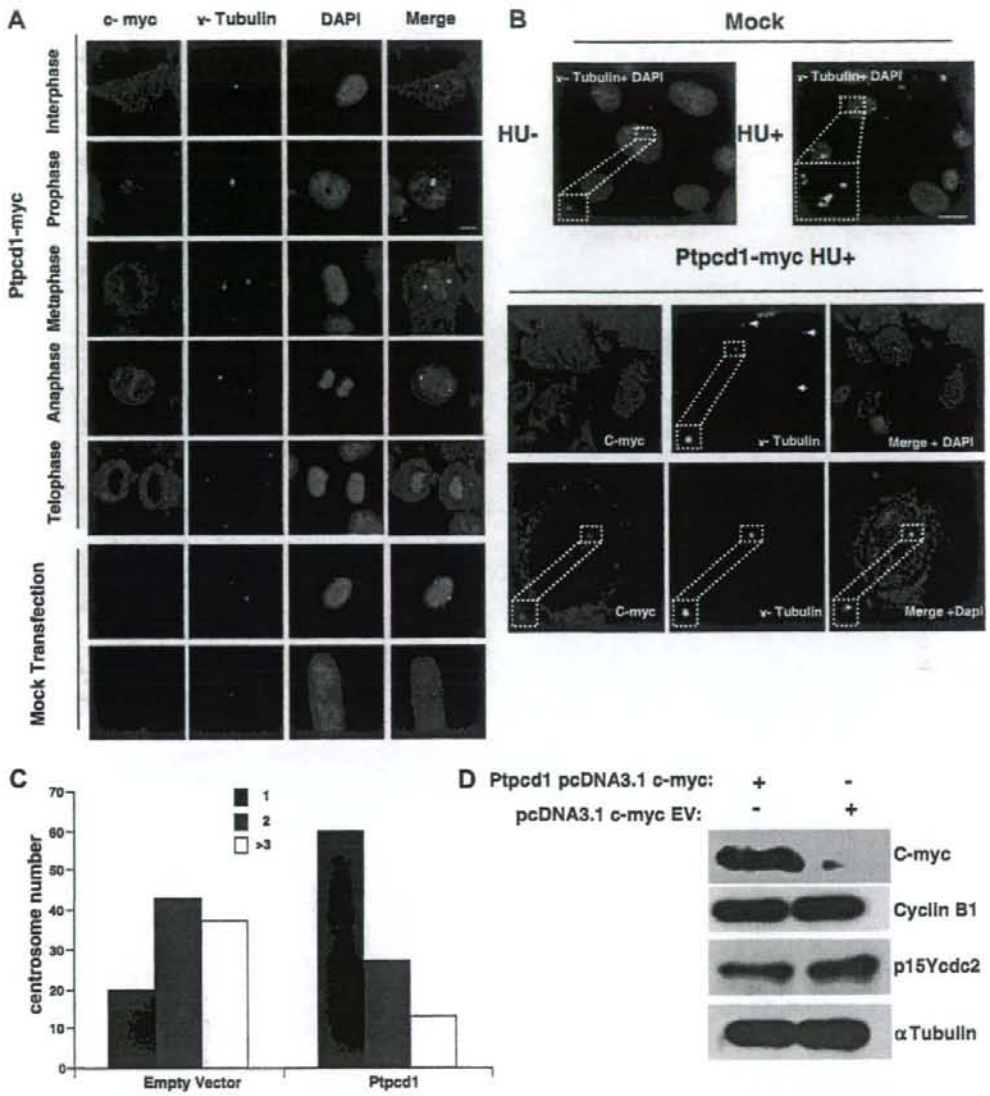

Fig. 1. Ptpcd1 localized to centrosomes and its overexpression prevents unscheduled centriole duplication. (A) Either Ptpcd1-myc or empty pcDNA3.1 as a negative control was transfected into HeLa cells. Cells were fixed with methanol and co-immunostained with γ-tubulin (green) and c-myc (red). DNA was counterstained with DAPI (blue). Scale bars; 5 μm. (B) Overexpression of Ptpcd1 prevents unscheduled centriole duplication. U2OS cells were transfected with either empty vector the presence or absence of HU (4 mM). (upper panels) or Ptpcd1-myc (lower panels) in the presence of HU (4 mM). Cells were then fixed and immunostained with anti-γ-tubulin antibodies (green) and c-myc (red). Arrows point at centrosomes, enlarged insets showed centrosomes. Scale bars; 5 μm. (C) The number of cells with 1, 2, or more than 2 centrosomes from (B) was counted and shown as a percentage of total cells. (D) Immunoblotting analysis. Whole cell extracts from (B) were subjected to immunoblotting using the indicate antibodies. (For interpretation of color mentioned in this figure the reader is referred to the web version of the article.)

ole, a microtubule depolymerizing agent. Overexpression of Ptpcd1-myc significantly stabilized microtubule organization when it was evaluated by staining with α-tubulin (Fig. 3D). Interestingly, it also enhanced microtubule regrowth after nocodazole washout. Thus, the effect of Ptpcd1-myc expression on microtubules stabilization was similar to that of Plk1 expression, further suggesting that Ptpcd1 functioned in Plk1-regulatory networks. In addition, these results also showed that the centrosomal localization of Ptpcd1 was independent of microtubules nucleation because centrosomal signals of Ptpcd1 could still be detected after microtubules depolymerization with nocodazole.

Overexpression of Ptpcd1 is capable of complementing prometaphase arrest in Plk1 depleted cells

We finally determined the genetic orientation between Plk1 and Ptpcd1. Endogenous Plk1 was depleted by the transfection of the specific siRNAs (D-1 and D-2) for Plk1. Immunoblotting using

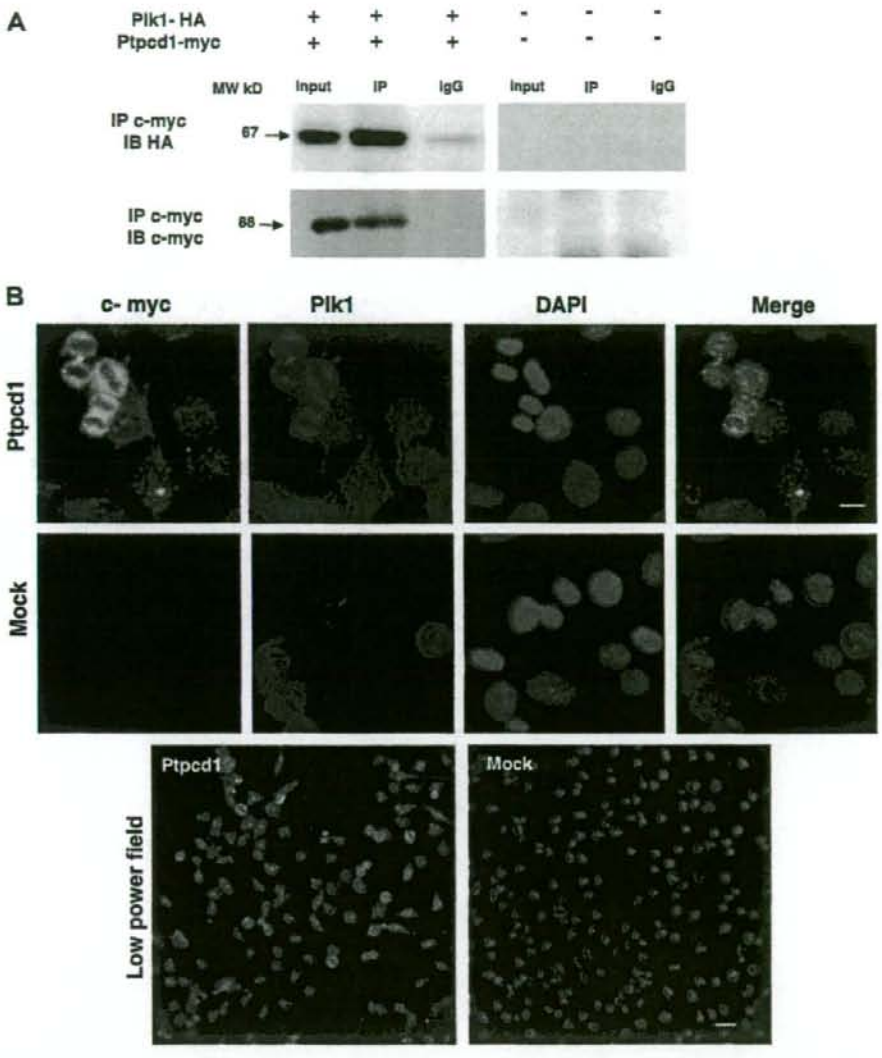

Fig. 2. Ptpcd1 interacted and colocalized with Plk1. U2OS cells were cotransfected with Plk1-HA and either Ptpcd1-myc or empty vectors (mock). Cells were harvested, and lysates were immunoprecipitated with anti-myc antibodies. Immunoprecipitates were subjected to immunoblotting using the indicated antibodies. (B) Colocalization of Ptpcd1 with Plk1. U2OS cells were transfected with Ptpcd1-myc and then stained with anti-myc antibodies (green) and anti-Plk1 antibodies (red, upper panels). DNA was counterstained with DAPI. Lower panels were low power fields of the upper images. Scale bars; 5 μm. (For interpretation of color mentioned in this figure the reader is referred to the web version of the article.)

anti-Plk1 antibodies revealed that transfection of D-1 and D-2 resulted in a significant reduction in Plk1 protein, whereas that of control siRNA did not (Fig. 4A). Plk1 depletion results in prometaphase/metaphase arrest [1], presumably due to impaired centrosomal separation, centrosome fragmentation, and microtubules destabilization, which consequently activate spindle checkpoints. Prolonged prometaphase arrest in Plk1 depleted cells ultimately appeared to induce apoptosis (Fig. 4B and Suppl. Fig. 2). Intriguingly, ectopic expression of Ptpcd1 in Plk1 depleted cells rescued the prometaphase/metaphase arrest and stabilized microtubules (Suppl. Fig. 2), but resulted in aberrant cytokinesis as was observed in Ptpcd1 expressing cells (Fig. 3C). These results indicated that Ptpcd1 at least in part functioned downstream of Plk1. Consistent with this notion, Ptpcd1 possessed four consensus serine residues for a Plk1 phosphorylation site (Fig. 4C) [26]. In this regard, Cdc5, a yeast homolog of Plks, regulated Cdc14p phosphorylation and its subcellular localization to ensure mitotic exit [14,27].

In summary, based on our observation in this study, it is possible that Ptpcd1 together with Plk1 may regulate the centriole duplication cycle as well as cytokinesis by modulating the phosphorylation status of some proteins, suggesting the conserved mechanism from yeast to mammalian by which Cdc5–Cdc14 axis regulates mitotic exit [1,14,27]. A similar counterbalance of kinase and phosphatase activities was also proposed in Nek2 and PP1α

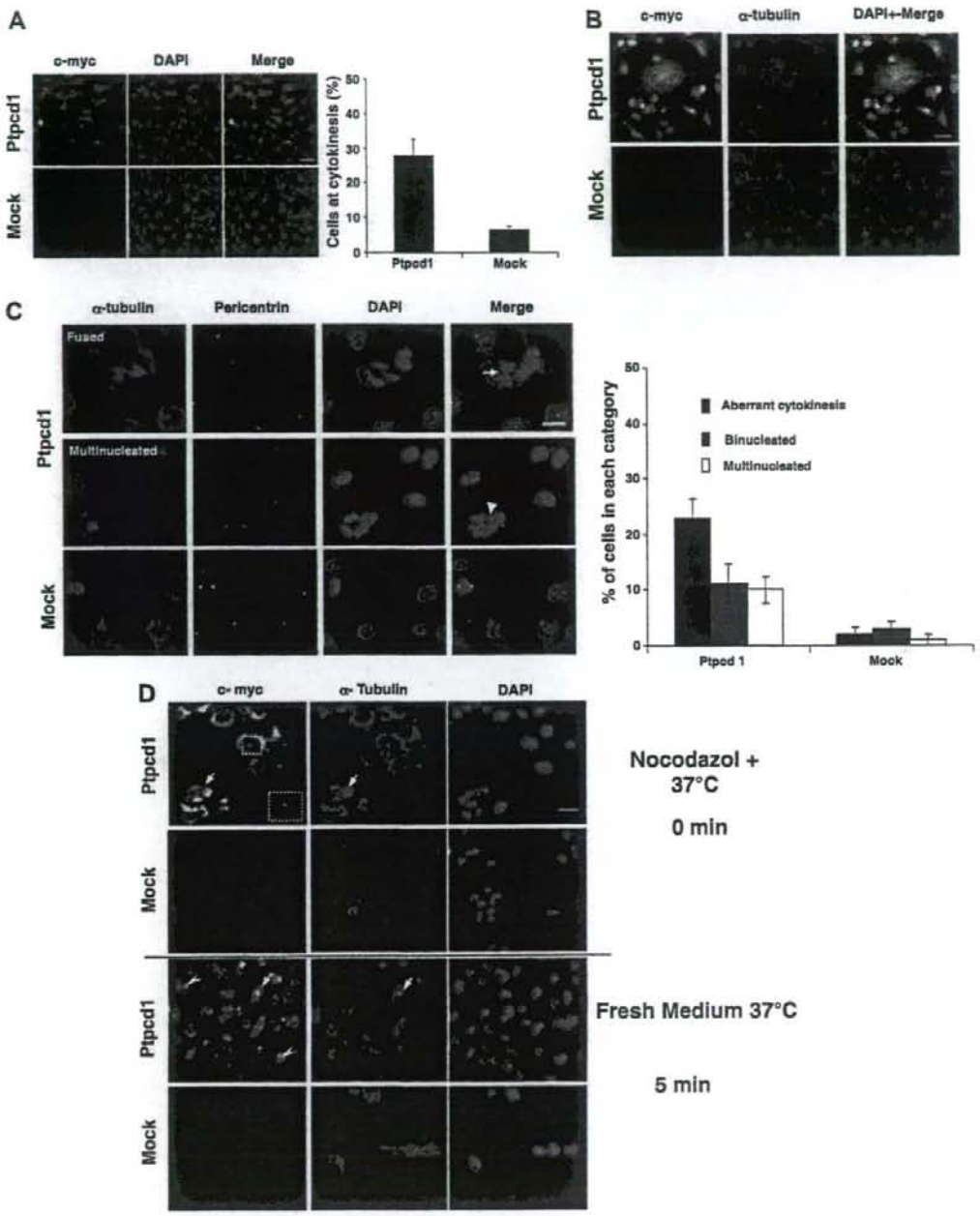

Fig. 3. Overexpression of Ptpcd1 resulted in aberrant cytokinesis and microtubules stabilization. (A) HeLa cells were transfected with either Ptpcd1-myc or empty vector (mock). Cells were immunostained with anti-myc (green) and DNA was counterstained with DAPI (blue). Scale bars; 5 μm (left panel). Cells with cytokinesis were counted and the data were presented as a percentage of total cells ($n > 200$) and means ± SD from three independent experiments (right panel). (B) HeLa cells were transfected as in (A) and stained with the indicated antibodies. DNA was counterstained with DAPI. (C) HeLa cells were transfected as in (B) and immunostained with anti-tubulin (red) and pericentrin (green). DNA was counterstained with DAPI. White arrow indicated persistent midbody structure and arrowhead pointed at multinucleated cells (left panels). Scale bars; 5 μm. Cells with aberrant cytokinesis, binucleated, and multinucleated cells from (left panels) were counted and the data were presented as a percentage of total cells ($n > 100$) and means ± SD from three independent experiments. (D) Microtubule regrowth assay. HeLa cells were transfected with either pcDNA3.1Ptpcd1-myc or empty vector. Cells were then treated with nocodazole as in Materials and Methods, and stained with anti-myc (green) and anti-α-tubulin (red) antibodies (upper panels). Cells were further cultured with the medium in the absence of nocodazole for 5 min and then stained as described above (lower panels). White arrow indicated stabilized α-tubulin bundles by Ptpcd1 and arrow head indicated newly growing microtubules. Insets show centrosomal Ptpcd1, Scale bars; 5 μm. (For interpretation of color mentioned in this figure the reader is referred to the web version of the article.)

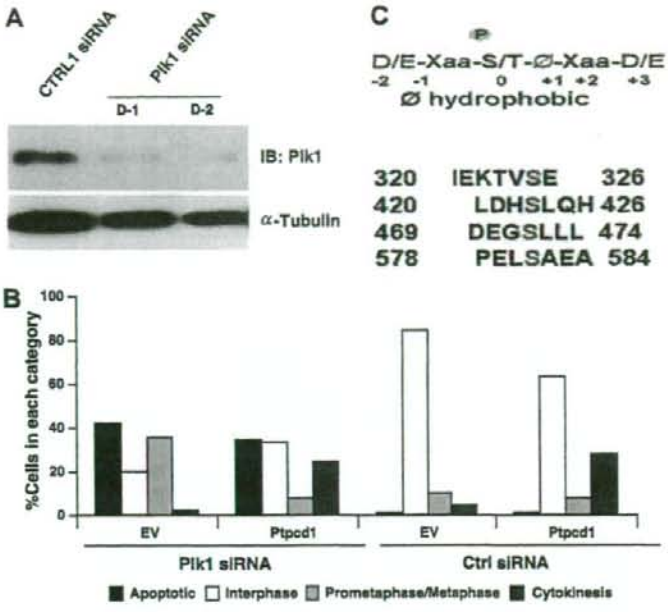

Fig. 4. Overexpression of Ptpcd1 rescued prometaphase/metaphase arrest observed in Plk1 depleted cells. (A) Plk1 depletion by transfection of its specific siRNAs. U2OS cells were transfected with the indicated siRNAs and the lysates were subjected to immunoblotting using the indicated antibodies. (B) U2OS cells were transfected with Ptpcd1 or empty vector (EV) as a negative control together with either Plk1 siRNA or control siRNA as indicated. The transfected cells were then fixed and immunostained stained with c-myc and α-tubulin. Cells in interphase, prometa/metaphase, cells with aberrant cytokinesis and/or underwent apoptosis were scored and the results were presented as a percentage of total cells ($n > 200$). (C) Schematic presentation of the predicted plk1 consensus phosphorylation site inside Ptpcd1 sequence. (For interpretation of color mentioned in this figure the reader is referred to the web version of the article.)

that governed centrosome splitting [4]. Although centrosomal and mitotic functions of mammalian Cdc14B had been described [15,17], Cdc14B deficient cells were viable and lacked apparent defects in chromosome segregation and cytokinesis [8], suggesting that alternative phosphatase(s) is being capable of complementing the mitotic functions of Cdc14B. Taken together with the fact that Ptpcd1 shared some sequence homology with Cdc14B, our results proposed that Ptpcd 1 might act as a functional isozyme to Cdc14B.

Acknowledgments

We thank Dr. Yamada-Namikawa for technical assistance and Dr. Majid Safwat for helpful discussion. This work was supported in part by the Ministry of Education, Science, Sports, and Culture of Japan through a Grant-in-Aid for Scientific Research (B) awarded to M.N.

Appendix A. Supplementary data

Supplementary data associated with this article can be found, in the online version, at doi:10.1016/j.bbrc.2009.01.113.

References

[1] T. Takaki, K. Trenz, V. Costanzo, M. Petronczki, Polo-like kinase 1 reaches beyond mitosis—cytokinesis, DNA damage response, and development, Curr. Opin. Cell Biol. 6 (2008) 650–660.
[2] L. Trinkle-Mulcahy, A.I. Lamond, Mitotic phosphatases: no longer silent partners, Curr. Opin. Cell Biol. 18 (2006) 623–631.
[3] K. Yuan, H. Hu, Z. Guo, G. Fu, A.P. Shaw, R. Hu, X. Yao, Phospho-regulation of HsCdc14A By polo-like kinase 1 is essential for mitotic progression, J. Biol. Chem. 282 (2007) 27414–27423.
[4] P. Meraldi, E.A. Nigg, Centrosome cohesion is regulated by a balance of kinase phosphatase activities, J. Cell Sci. 114 (2001) 3749–3757.
[5] C.G. Pearson, B.P. Culver, M. Winey, Centrioles want to move out and make cilia, Dev. Cell 13 (2007) 319–321.
[6] N. R Helps, X. Luo, H.M. Barker, P.T. Cohen, NIMA-related kinase 2 (Nek2), a cell cycle-regulated protein kinase localized to centrosomes, is complexed to protein phosphatase 1, Biochem. J. 349 (2000) 509–518.
[7] B.M. Lange, Integration of the centrosome in cell cycle control, stress response and signal transduction pathways, Curr. Opin. Cell Biol. 14 (2002) 35–43.
[8] P. Meraldi, J. Lukas, A.M. Fry, J. Bartek, E.A. Nigg, Centrosome duplication in mammalian somatic cells requires E2F and Cdk2-cyclin A, Nat. Cell Biol. 1 (1999) 88–93.
[9] F.A. Barr, H.H. Silljé, E.A. Nigg, Polo-like kinases and the orchestration of cell division, Nat. Rev. Mol. Cell Biol. 5 (2004) 429–440.
[10] I. Sumara, J.F. Gimenez-Abian, D. Gerlich, T. Hirota, C. Kraft, C. de la Torre, J. Ellenberg, J.M. Peters, Roles of polo-like kinase 1 in the assembly of functional mitotic spindles, Curr. Biol. 14 (2004) 1712–1722.
[11] P. Lenart, M. Petronczki, M. Steegmaier, B. Di Fiore, J.J. Lipp, M. Hoffmann, W.J. Rettig, N. Kraut, J.M. Peters, The small molecule inhibitor BI 2536 reveals novel insights into mitotic roles of polo-like kinase 1, Curr. Biol. 17 (2007) 304–315.
[12] M. Petronczki, M. Glotzer, N. Kraut, J.M. Peters, Polo-like kinase 1 triggers the initiation of cytokinesis in human cells by promoting recruitment of the RhoGEF Ect2 to the central spindle, Dev. Cell 12 (2007) 713–725.
[13] R. Neef, U. Gruneberg, R. Kopajtich, X. Li, E.A. Nigg, H. Silljé, F.A. Barr, Choice of Plk1 docking partners during mitosis and cytokinesis is controlled by the activation state of Cdk1, Nat. Cell Biol. 9 (2007) 436–444.
[14] R. Visintin, F. Stegmeier, A. Amon, The role of the polo kinase Cdc5 in controlling Cdc14 localization, Mol. Biol. Cell 14 (2003) 4486–4498.
[15] J. Wu, H.P. Cho, D.B. Rhee, D.K. Johnson, J. Dunlap, Y. Liu, Y. Wang, Cdc14B depletion leads to centriole amplification, and its overexpression prevents unscheduled centriole duplication, J. Cell Biol. 181 (2008) 475–483.
[16] B.K. Kaiser, Z.A. Zimmerman, H. Charbonneau, P.K. Jackson, Disruption of centrosome structure, chromosome segregation, and cytokinesis by misexpression of human Cdc14A phosphatase, Mol. Biol. Cell 13 (2002) 2289–2300.
[17] H.P. Cho, Y. Liu, M. Gomez, J. Dunlap, M. Tyers, Y. Wang, The dual-specificity phosphatase CDC14B bundles and stabilizes microtubules, Mol. Cell Biol. 25 (2005) 4541–4551.
[18] E. Berdougo, M.V. Nachury, P.K. Jackson, P.V. Jallepalli, The nucleolar phosphatase Cdc14B is dispensable for chromosome segregation and mitotic exit in human cells, Cell Cycle 7 (2008) 1184–1190.

[19] T. Matsui, Y. Katsuno, T. Inoue, F. Fujita, T. Joh, H. Niida, H. Murakami, M. Itoh, M. Nakanishi, Negative regulation of Chk2 expression by p53 is dependent on the CCAAT-binding transcription factor NF-Y, J. Biol. Chem. 279 (2004) 25093–250100.
[20] M. Shimada, H. Niida, D.H. Zineldeen, H. Tagami, M. Tanaka, H. Saito, M. Nakanishi, Chk1 is a histone H3 threonine 11 kinase that regulates DNA damage-induced transcriptional repression, Cell 132 (2008) 221–232.
[21] H. Niida, Y. Katsuno, B. Banerjee, M.P. Hande, M. Nakanishi, Specific role of Chk1 phosphorylations in cell survival and checkpoint activation, Mol. Cell Biol. 27 (2007) 2572–2581.
[22] O.V. Plotnikova, E.A. Golemis, E.N. Pugacheva, Cell cycle-dependent ciliogenesis and cancer, Cancer Res. 68 (2008) 2058–2061.
[23] A. Spektor, W.Y. Tsang, D. Khoo, B.D. Dynlacht, Cep97 and CP110 suppress a cilia assembly program, Cell 130 (2007) 678–690.
[24] L.M. Quarmby, M.R. Mahjoub, Caught Nek-ing: cilia and centrioles, J. Cell Sci. 118 (2005) 5161–5169.
[25] T.S. McClintock, C.E. Glasser, S.C. Bose, D.A. Bergman, Tissue expression patterns identify mouse cilia genes, Physiol. Genomics 32 (2008) 198–206.
[26] H. Nakajima, F. Toyoshima-Morimoto, E. Taniguchi, E. Nishida, Identification of a consensus motif for Plk (Polo-like kinase) phosphorylation reveals Myt1 as a Plk1 substrate, J. Biol. Chem. 278 (2003) 25277–25280.
[27] C. Visintin, B.N. Tomson, R. Rahal, J. Paulson, M. Cohen, J. Taunton, A. Amon, R. Visintin, APC/C-Cdh1-mediated degradation of the Polo kinase Cdc5 promotes the return of Cdc14 into the nucleolus, Genes Dev. 22 (2008) 79–90.

Biochemical and Biophysical Research Communications 374 (2008) 79–83

Contents lists available at ScienceDirect

Biochemical and Biophysical Research Communications

journal homepage: www.elsevier.com/locate/ybbrc

Essential role of Chk1 in S phase progression through regulation of RNR2 expression

Hiromichi Naruyama [a,b], Midori Shimada [a], Hiroyuki Niida [a], Doaa H. Zineldeen [a], Yoshihiro Hashimoto [b], Kenjiro Kohri [b], Makoto Nakanishi [a,*]

[a] Department of Cell Biology, Graduate School of Medical Sciences, Nagoya City University, 1 Kawasumi, Mizuho-cho, Mizuho-ku, Nagoya 467-8601, Japan
[b] Department of Urology, Graduate School of Medical Sciences, Nagoya City University, 1 Kawasumi, Mizuho-cho, Mizuho-ku, Nagoya 467-8601, Japan

ARTICLE INFO

Article history:
Received 24 June 2008
Available online 9 July 2008

Keywords:
Cell cycle
Ribonucleotide reductase
Chk1
Transcription
DNA replication

ABSTRACT

Chk1 is an essential kinase for maintaining genome integrity and cell cycle checkpoints through phosphorylating several downstream targets. Recently, we demonstrated that Chk1 is also required for cell proliferation in somatic cells under unperturbed condition through regulating transcription of several genes. Here, we show that Chk1 is required for S phase progression and RNR2 is a critical downstream target of genes transcriptionally regulated by Chk1. Hence, although RNR2 expression reached maximum at S phase in the presence of Chk1, Chk1 depletion arrested the cell cycle at S phase and reduced RNR2 expression at both mRNA and protein levels. Ectopic expression of RNR2 failed to rescue the S phase arrest observed in Chk1 depleted cells, suggesting the presence of an additional Chk1-target(s) for completion of S phase other than RNR2. Therefore, our results suggest that Chk1 is required for DNA replication at least through regulating RNR2 gene transcription.

© 2008 Elsevier Inc. All rights reserved.

Progression through the cell cycle is regulated carefully to avoid proliferation or mitosis when adverse conditions exist, such as DNA damage and DNA replication fork stalling [1–3]. Abnormal DNA structures are rapidly sensed and transduced to mediators by either the ATR or ATM PI3-kinase related protein kinases (PIKK) [4,5]. One such mediator is Chk1 kinase that is essential for cell cycle arrest upon DNA damage or DNA replication fork stalling through phosphorylating Cdc25 phosphatases [6,7]. In addition to its role as a checkpoint mediator, Chk1 is a constitutively active enzyme and associates with chromatin under unperturbed condition [8,9]. Chk1 phosphorylates histone H3 at threonine 11 (T11) around the promoter regions of cell cycle regulatory genes including cyclin B1 and Cdk1 [10], which accelerate recruitment of GCN5 histone acetyltransferase and subsequent acetylation at lysine 9 (K9) [11]. Increased acetylation of K9 leads to transcriptional activation.

Ribonucleotide reductase (RNR) is essential for de novo synthesis of deoxyribonucleotides (dNTPs), which are required for DNA replication and repair [12,13]. Most eukaryotic RNRs are composed of two essential and non-identical homodimeric subunits, a large subunit (R1) and a small subunit (R2) [12,14]. The former subunit contains the catalytic site and allosteric regulatory site for both enzyme activity and specificity by binding nucleotide triphosphates [12]. The latter subunit contains a non-heme iron center essential for catalysis. p53-Inducible R2 (53R2) [15], a homologous R2 protein, is also capable of forming an active RNR complex together with the R1 protein [16].

In mammalian cells, the transcription of the R1 and R2 genes is cell cycle dependent, being undetectable in G0/G1 and maximum in S phase [17,18]. The S phase-specific expression of R1 genes is characterized as four different promoter elements, b, a, Inr, and g [19]. Although transcription factor YY1 binds to b and a elements, the cell cycle specific expression is mainly regulated via Inr and g elements. In contrast to R1, the S phase specific expression of R2 is relatively complicated. In mouse cells, S phase-specific transcription of R2 gene requires a repressive E2F-binding site and a promoter-activating region [20]. Interestingly, mutation of the E2F-binding site leads to premature promoter activation in G1 and increase promoter activity. Given that the R1 protein has a long half-life, and its level is apparently constant [21,22] and that the R2 protein is rapidly degraded in mitosis by APC-C [23,24], RNR activity and thus DNA replication are mainly dependent on the level of R2 protein.

In this study, we found that Chk1 depletion results in incomplete S phase, suggesting that Chk1 may be required for transcription of some essential genes for DNA replication. To address this question, we examined changes in the transcription of known genes involved in S phase progression after Chk1 depletion in MEFs. Only

* Corresponding author. Address: Department of Cell Biology, Graduate School of Medical Sciences, Nagoya City University, Kawasumi, Mizuho-cho, Mizuho-ku, Nagoya 467-8601, Japan. Fax: +81 52 842 3955.
E-mail address: mkt-naka@med.nagoya-cu.ac.jp (M. Nakanishi).

0006-291X/$ - see front matter © 2008 Elsevier Inc. All rights reserved.
doi:10.1016/j.bbrc.2008.06.112

RNR2 among genes tested was drastically reduced following loss of Chk1. Therefore, our results suggest an essential function of Chk1 in DNA replication at least through activating RNR2 gene transcription.

Materials and methods

Cells and culture condition. Chk1$^{flox/-}$ MEFs were generated as described previously [10] and were cultured in DMEM supplemented with 10% FBS.

Immunoblotting. Cells were lysed as described previously [10], and extracts were subjected to immunoblotting using anti-Chk1 (sc8408; Santa Cruz), anti-RNR2 (sc10844; Santa Cruz), anti-RNR1 (sc11733; Santa Cruz) antibodies.

Northern blotting. Total RNA was extracted using ISOGEN (Wako) and northern blotting was performed as described previously [25]. ^{32}P-labeled fragment of RNR2 and RNR1 was used as a probe.

Cell cycle analysis. Cells were incubated with 10 μM BrdU for 30 min, harvested, washed once in PBS and fixed with in 70% ethanol. Cells were prepared for FACS analysis as described previously [26].

Real time PCR. Real-time PCR was carried out with single-stranded cDNAs prepared with the SuperScript First-Strand Synthesis System (Invitrogen, Carlsbad, CA, USA). Briefly, total RNA from each sample after transfection was reverse-transcribed with Oligo-DT primer. PCR reactions were performed with Power SYBR Green PCR Master Mix and 7500 Fast Real-Time PCR System (Applied Biosystems, Foster City, CA, USA). Seuence-Specific primers were designed by Primer3 software (http://frodo.wi.mit.edu/cgi-bin/primer3/primer3_www.cgi) as follows; GAPDH, AAC TTTGGCATTGTGGAAGG and GGATGCAGGGATGATGTTCT, Asf1, CAG GCCATTTTACCTTCAGC and GGCTGAGCTTGTTTCTGGAC, MCM4, GACCCTCAGGATGAGGCATA and GGGGCATGATGGTACTATGG, Cdc25C, AAAGACAGGGCTCTGAACCA and TGGTGAAGCATGGGAC AGTA, RNR1, GGTCGTGTCCGAAAAGTTGT and GTTCTGCTGGTTG CTCTTCC RNR2, CGTTGTCTTTCCCATCGAGT and CTCTCATCGGG TTTCAGAGC, Cdc7, GCCCTGCAGAGAAACTCATC and GTTTCCCTC ATCACGCTGTT, Cdc6, TTTCGGAAGTTGATGGGAAC and GGGTCAA AAGCAGCAAAGAG Orc1, ACTGCCATACCCAACCATGT and CAGCA CGTCATTCTGGCTAA, Orc2, TTTGTGCCTTCCTTTTCTGC and CCCA AG CCATAAAGCACAAT, Wee1, GAGAGCTGGAGGACGACTTG and CAGAA AGTAGGCGGTCGAAG, Cdc45, GTTCCTGCCTACGACGACAT and CTC TTCCTGTTTCGCTCCAC. GAPDH primer was used as an internal control. Real-Time PCR was carried out, in duplicate, by 40 cycles of 95 °C for 10 sec and 60 °C for 1 min. Productions of the expected amplification fragments without unanticipated products and primers were confirmed by melting-curve analysis. To determine the relative amounts of the products, we used the comparative Ct (threshold cycle) method according to the instructions supplied by Applied Biosystems. Conventional PCR was performed with the Ex-Taq system (Takara Bio Inc., Shiga, Japan).

Immunohistochemical analysis. Chk1$^{flox/-}$ MEFs were infected with adenoviruses expressing either Cre or LacZ (negative control). Immunohistochemical analyses using anti-RNR1 and anti-RNR2 antibodies were performed as described previously [9].

Results and discussion

Loss of Chk1 resulted in incomplete DNA replication

Recent findings that Chk1 is a histone H3-T11 kinase unravel a mechanism underlying DNA damage-induced transcriptional repression. In this concept, Chk1 is an essential for transcription of some genes under unperturbed condition. Actually, Chk1 depletion in

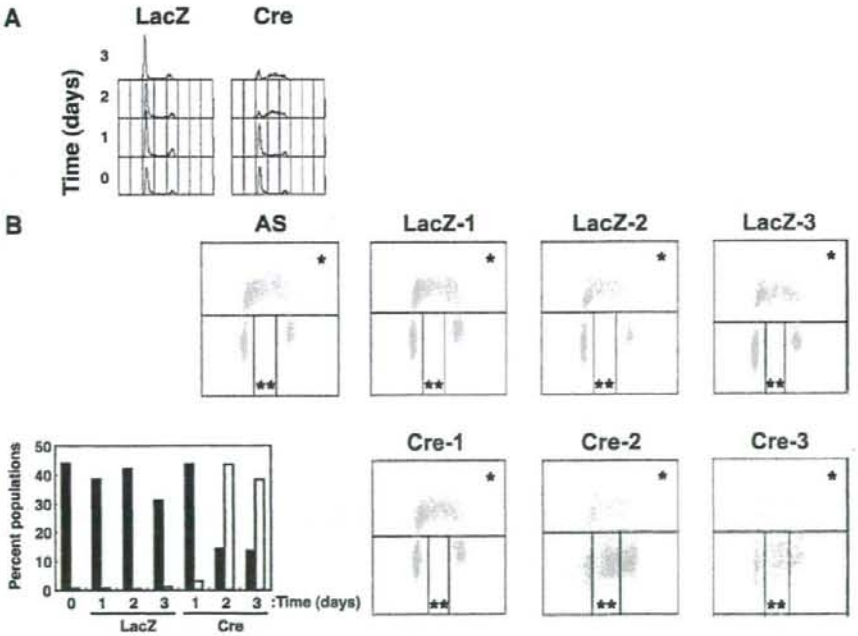

Fig. 1. Chk1 depleted MEFs show S phase arrest. (A) Cell cycle profile of Chk1$^{flox/-}$ and Chk1$^{Δ/-}$ MEFs at the indicated days after adenoviral infection. (B) Chk1$^{flox/-}$ MEFs were treated with 10 μM BrdU for 30 min before cells were harvested at the time indicated after infection and analysed by FACS. The percentages of BrdU positive (*) and negative (**) cells are shown as a graph (black: BrdU positive; white: BrdU negative).

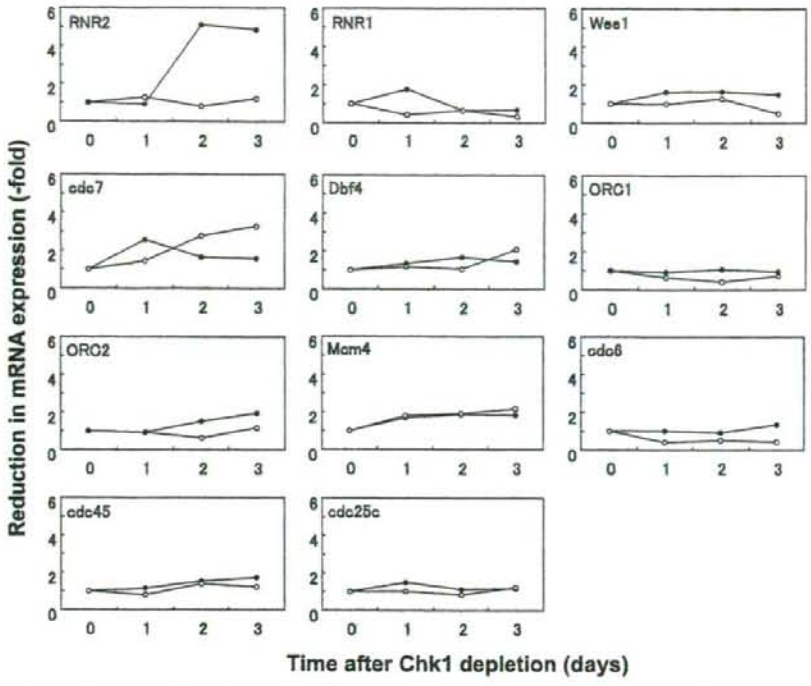

Fig. 2. RNR2 mRNA transcripts were decreased in Chk1 depleted MEFs. Chk1$^{flox/-}$ MEFs were harvested at the indicated times after infection of adenoviruses expressing LacZ (open circles) or Cre (closed circles) and their total RNA was extracted. After treatment with reverse transcriptase using random primers, real time PCR was performed using their specific primers to measure the transcripts involved in DNA replication or cell cycle control. The results are presented as a fold-reduction of controls (before infection of adenoviruses).

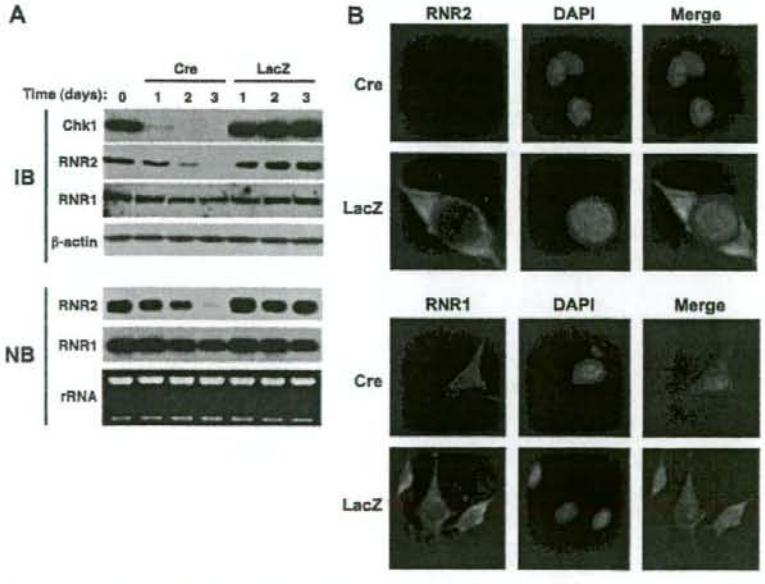

Fig. 3. Specific reduction in RNR2 protein in Chk1 depleted MEFs. Chk1$^{flox/-}$ MEFs were harvested at the indicated times after infection of adenoviruses expressing LacZ or Cre. The resultant whole cell extracts and total RNA were prepared and subjected to immunoblotting (IB) using the indicated antibodies or northern blotting (NB) analysis using RNR2 or RNR1 probes. (B) Immunohistochemical analysis of RNR2 and RNR1 in Chk1 depleted cells. Chk1$^{flox/-}$ MEFs were infected with adenoviruses expressing either LacZ or Cre. Three days after infection the resultant cells were fixed and stained with anti-RNR2 or anti-RNR1 antibodies. Cells were also counterstained with DAPI.

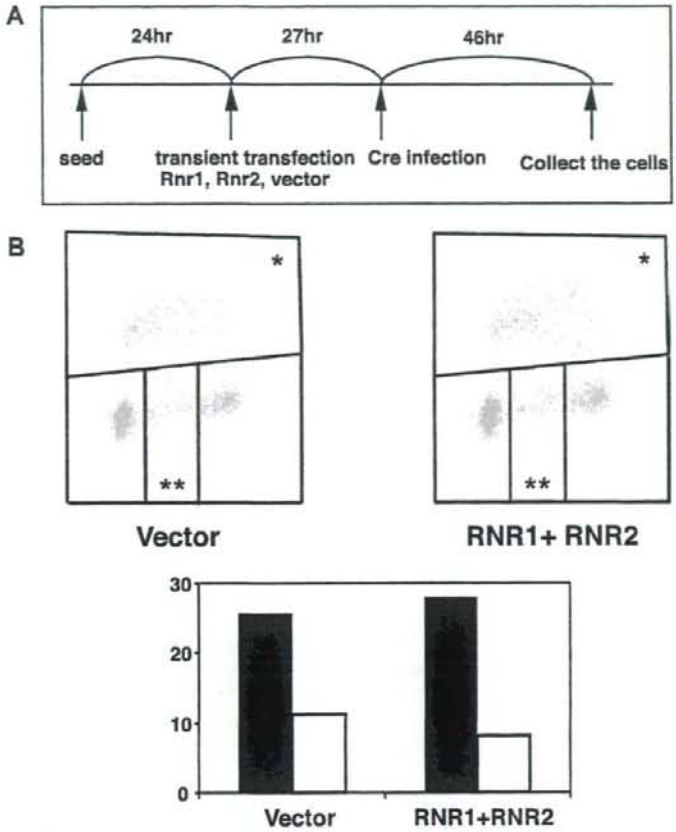

Fig. 4. Ectopic expression of RNR2 and RNR1 is insufficient for complement S phase arrest in Chk1 depleted MEFs. (A) Time course strategy for transient transfection of RNR2 and RNR1, and Chk1 depletion by Ade-Cre infection. (B) BrdU staining and FACS analysis were performed as indicated in Fig. 1. The percentages of each cell cycle distribution were also shown (black: BrdU positive; white: BrdU negative).

somatic cells by infection of adenoviruses expressing Cre reduced expression of more than 200 transcripts [10]. Therefore, increased S phase population in Chk1 depleted MEFs (Fig. 1A) are likely due to S phase arrest but not enhanced initiation of DNA replication. To address this question, we first examined BrdU incorporation in Chk1 depleted MEFs. After infection of adenoviruses expressing Cre, $Chk1^{del/-}$ MEFs were incubated with culture medium containing 10 μM BrdU for 30 min. Cells were then fixed, immunostained with anti-BrdU antibodies, and analyzed by FACScan. As shown in Fig. 1B, majority of S phase cells in control MEFs were BrdU positive and infection of adenoviruses expressing LacZ did not affect cell cycle progression. In contrast, although most of S phase cells in $Chk1^{del/-}$ MEFs were BrdU positive at 1 day after adenoviral infection, they became negative at two days or thereafter, indicating that increased S phase population is due to S phase arrest.

Transcriptional changes in genes involved in DNA replication after Chk1 depletion

We next examined the changes in the expression of genes involved in DNA replication after Chk1 depletion. Quantitative real time PCR revealed that the expression of RNR2, but not RNR1, was significantly reduced at two days after Chk1 depletion, whereas those of the other genes tested were almost constant during this experimental period (Fig. 2). Given that expression of many genes involved in RNR2, ASK, ORC1, cdc6, and cdc25c were dependent on the functional E2Fs [20,27–30], reduction in RNR2 expression was not likely due to the impairment of E2F functions. In addition, because RNR2 expression is cell cycle dependent, reaching at a maximum at S phase [20], decreased expression of RNR2 did not solely reflect the changes in cell cycle profile following Chk1 depletion (Fig. 1A).

The reduction in RNR2 protein as well as its mRNA was also confirmed by northern blotting, immunoblotting, and immunohistochemistry using specific antibodies to RNR2, respectively (Fig. 3A and B). The reduction in RNR2 protein was obvious at two days after Chk1 depletion, supporting the observation that S phase arrest in Chk1 depleted cells was detected at two days after infection. RNR2 was predominantly localized at cytoplasm and RNR1 was localized at both cytoplasm and nucleus, consistent with the previous reports [12], but signal of RNR2, but not RNR1, was almost disappeared after Chk1 depletion. Thus, S phase arrest following Cre infection appeared to be correlated well with the reduction in RNR2 protein.

Ectopic expression of RNR2 is not sufficient for complement S phase arrest in $Chk1^{del/-}$ MEFs

We finally asked whether ectopic expression could reverse the S phase arrest in $Chk1^{del/-}$ MEFs. Experimental protocols were

summarized in Fig. 4A. In brief, MEFs were transfected with both expression vectors for RNR1 and RNR2 and then infected with Cre. Forty six hours after infection, cells were incubated with the medium containing 10 μM BrdU and analyzed by FACScan. As shown in Fig. 4B, coexpression of RNR1 and RNR2 was not capable of reducing BrdU negative S phase population. These results suggests that ectopic expression of RNR1 and RNR2 is not sufficient for rescue the S phase arrest in Chk1 deficient MEFs and thus existence of unidentified transcriptional targets of Chk1 which is essential for completion of DNA replication. Clearly, additional work is necessary to clarify those Chk1 targets and their role in S phase progression.

Acknowledgments

We thank Dr. Yamada-Namikawa for discussion and technical assistance. This work was supported in part by the Ministry of Education, Science, Sports, and Culture of Japan through a Grant-in-Aid for Scientific Research (B) awarded to M.N.

References

[1] M. Nakanishi, M. Shimada, H. Niida, Genetic instability in cancer cells by impaired cell cycle checkpoints, Cancer Sci. 97 (2006) 984–989.
[2] M. Shimada, M. Nakanishi, DNA damage checkpoints and cancer, J. Mol. Histol. 37 (2006) 253–260.
[3] J.W. Harper, S.J. Elledge, The DNA damage response: ten years after, Mol. Cell. 28 (2007) 739–745.
[4] R.T. Abraham, Cell cycle checkpoint signaling through the ATM and ATR kinases, Genes Dev. 15 (2001) 2177–2196.
[5] Y. Shiloh, ATM and related protein kinases: safeguarding genome integrity, Nat. Rev. Cancer 3 (2003) 155–168.
[6] Y. Sanchez, C. Wong, R.S. Thoma, R. Richman, Z. Wu, H. Piwnica-Worms, S.J. Elledge, Conservation of the Chk1 checkpoint pathway in mammals: linkage of DNA damage to Cdk regulation through Cdc25, Science 277 (1997) 1497–1501.
[7] C.Y. Peng, P.R. Graves, R.S. Thoma, Z. Wu, A.S. Shaw, H. Piwnica-Worms, Mitotic and G2 checkpoint control: regulation of 14-3-3 protein binding by phosphorylation of Cdc25C on serine-216, Science 277 (1997) 1501–1505.
[8] V.A. Smits, P.M. Reaper, S.P. Jackson, Rapid PIKK-dependent release of Chk1 from chromatin promotes the DNA-damage checkpoint response, Curr. Biol. 16 (2006) 150–159.
[9] H. Niida, Y. Katsuno, B. Banerjee, M.P. Hande, M. Nakanishi, Specific role of Chk1 phosphorylations in cell survival and checkpoint activation, Mol. Cell. Biol. 27 (2007) 2572–2581.
[10] M. Shimada, H. Niida, D.H. Zineldeen, H. Tagami, M. Tanaka, H. Saito, M. Nakanishi, Chk1 is a Histone H3 Threonine 11 kinase that regulates DNA damage-induced transcriptional repression, Cell 132 (2008) 221–232.
[11] J.E. Brownell, J. Zhou, T. Ranalli, R. Kobayashi, D.G. Edmondson, S.Y. Roth, C.D. Allis, Tetrahymena histone acetyltransferase A: a homolog to yeast Gcn5p linking histone acetylation to gene activation, Cell 84 (1996) 843–851.
[12] P. Nordlund, P. Reichard, Ribonucleotide reductases, Annu. Rev. Biochem. 75 (2006) 681–706.
[13] A. Chabes, B. Georgieva, V. Domkin, X. Zhao, R. Rothstein, L. Thelander, Survival of DNA damage in yeast directly depends on increased dNTP levels allowed by relaxed feedback inhibition of ribonucleotide reductase, Cell 112 (2003) 391–401.
[14] J. Stubbe, J. Ge, C.S. Yee, The evolution of ribonucleotide reduction revisited, Trends Biochem. Sci. 26 (2001) 93–99.
[15] H. Tanaka, H. Arakawa, T. Yamaguchi, K. Shiraishi, S. Fukuda, K. Matsui, Y. Takei, Y. Nakamura, A ribonucleotide reductase gene involved in a p53-dependent cell-cycle checkpoint for DNA damage, Nature 404 (2000) 42–49.
[16] O. Guittet, P. Hakansson, N. Voevodskaya, S. Fridd, A. Graslund, H. Arakawa, Y. Nakamura, L. Thelander, Mammalian p53R2 protein forms an active ribonucleotide reductase in vitro with the R1 protein, which is expressed both in resting cells in response to DNA damage and in proliferating cells, J. Biol. Chem. 276 (2001) 40647–40651.
[17] S. Bjorklund, S. Skog, B. Tribukait, L. Thelander, S-phase-specific expression of mammalian ribonucleotide reductase R1 and R2 subunit mRNAs, Biochemistry 29 (1990) 5452–5458.
[18] M. Hengstschlager, I. Mudrak, E. Wintersberger, E. Wawra, A common regulation of genes encoding enzymes of the deoxynucleotide metabolism is lost after neoplastic transformation, Cell Growth Differ. 5 (1994) 1389–1394.
[19] E. Johansson, K. Hjortsberg, L. Thelander, Two YY-1-binding proximal elements regulate the promoter strength of the TATA-less mouse ribonucleotide reductase R1 gene, J. Biol. Chem. 273 (1998) 29816–29821.
[20] A.L. Chabes, S. Bjorklund, L. Thelander, S Phase-specific transcription of the mouse ribonucleotide reductase R2 gene requires both a proximal repressive E2F-binding site and an upstream promoter activating region, J. Biol. Chem. 279 (2004) 10796–10807.
[21] S. Eriksson, A. Graslund, S. Skog, L. Thelander, B. Tribukait, Cell cycle-dependent regulation of mammalian ribonucleotide reductase. The S phase-correlated increase in subunit M2 is regulated by de novo protein synthesis, J. Biol. Chem. 259 (1984) 11695–11700.
[22] Y. Engstrom, S. Eriksson, I. Jildevik, S. Skog, L. Thelander, B. Tribukait, Cell cycle-dependent expression of mammalian ribonucleotide reductase. Differential regulation of the two subunits, J. Biol. Chem. 260 (1985) 9114–9116.
[23] A. Chabes, L. Thelander, Controlled protein degradation regulates ribonucleotide reductase activity in proliferating mammalian cells during the normal cell cycle and in response to DNA damage and replication blocks, J. Biol. Chem. 275 (2000) 17747–17753.
[24] A.L. Chabes, C.M. Pfleger, M.W. Kirschner, L. Thelander, Mouse ribonucleotide reductase R2 protein: a new target for anaphase-promoting complex-Cdh1-mediated proteolysis, Proc. Natl. Acad. Sci. USA 100 (2003) 3925–3929.
[25] M. Shimada, C. Namikawa-Yamada, M. Nakanishi, H. Murakami, Regulation of Cdc2p and Cdc13p is required for cell cycle arrest induced by defective RNA splicing in fission yeast, J. Biol. Chem. 280 (2005) 32640–32648.
[26] M. Zhu, R.S. Weiss, Increased common fragile site expression, cell proliferation defects, and apoptosis following conditional inactivation of mouse Hus1 in primary cultured cells, Mol. Biol. Cell 18 (2007) 1044–1055.
[27] Z. Kherrouche, A. Blais, E. Ferreira, Y. De Launoit, D. Monte, ASK-1 (apoptosis signal-regulating kinase 1) is a direct E2F target gene, Biochem. J. 396 (2006) 547–556.
[28] K. Ohtani, J. DeGregori, G. Leone, D.R. Herendeen, T.J. Kelly, J.R. Nevins, Expression of the HsOrc1 gene, a human ORC1 homolog, is regulated by cell proliferation via the E2F transcription factor, Mol. Cell. Biol. 16 (1996) 6977–6984.
[29] K. Ohtani, A. Tsujimoto, M. Ikeda, M. Nakamura, Regulation of cell growth-dependent expression of mammalian CDC6 gene by the cell cycle transcription factor E2F, Oncogene 17 (1998) 1777–1785.
[30] U. Haugwitz, M. Wasner, M. Wiedmann, K. Spiesbach, K. Rother, J. Mossner, K. Engeland, A single cell cycle genes homology region (CHR) controls cell cycle-dependent transcription of the cdc25C phosphatase gene and is able to cooperate with E2F or Sp1/3 sites, Nucleic Acids Res. 30 (2002) 1967–1976.

Cell

Chk1 Is a Histone H3 Threonine 11 Kinase that Regulates DNA Damage-Induced Transcriptional Repression

Midori Shimada,[1] Hiroyuki Niida,[1] Doaa H. Zineldeen,[1] Hideaki Tagami,[2] Masafumi Tanaka,[3] Hiroyuki Saito,[3] and Makoto Nakanishi[1,*]
[1]Department of Cell Biology and Biochemistry, Graduate School of Medical Sciences
[2]Graduate School of Natural Sciences
Nagoya City University, 1 Kawasumi, Mizuho-cho, Mizuho-ku, Nagoya 467-8601, Japan
[3]Laboratory of Biophysical Chemistry, Kobe Pharmaceutical University, Motoyama Kita-machi, Higashinada-ku, Kobe 658-8558, Japan
*Correspondence: mkt-naka@med.nagoya-cu.ac.jp
DOI 10.1016/j.cell.2007.12.013

SUMMARY

DNA damage results in activation or suppression of transcription of a large number of genes. Transcriptional activation has been well characterized in the context of sequence-specific DNA-bound activators, whereas mechanisms of transcriptional suppression are largely unexplored. We show here that DNA damage rapidly reduces histone H3 Threonine 11 (T11) phosphorylation. This correlates with repression of genes, including *cyclin B1* and *cdk1*. H3-T11 phosphorylation occurs throughout the cell cycle and is Chk1 dependent in vivo. Following DNA damage, Chk1 undergoes rapid chromatin dissociation, concomitant with reduced H3-T11 phosphorylation. Furthermore, we find that loss of H3-T11 phosphorylation correlates with reduced binding of the histone acetyltransferase GCN5 at *cyclin B1* and *cdk1* promoters and reduced H3-K9 acetylation. We propose a mechanism for Chk1 as a histone kinase, responsible for DNA-damage-induced transcriptional repression by loss of histone acetylation.

INTRODUCTION

In eukaryotes, DNA damage alters the global patterns of gene expression to orchestrate a variety of cellular events including growth arrest, apoptosis, and DNA repair. Following ultraviolet (UV)-induced DNA damage ~4% of transcripts show >3 fold-changes. Approximately 90% represent downregulation (Gentile et al., 2003). Unlike transcriptional activation, transcriptional repression after DNA damage has been largely unexplored.

Targeted covalent modification of the amino-terminal tails of core histones is an important mechanism regulating RNA polymerase II-dependent transcription. The enzymes that catalyze histone lysine acetylation are known as histone acetyltransferases (HATs). The GCN5 family represent the first identified nuclear HATs (Brownell et al., 1996), and GCN5 is present in at least four high-molecular-weight complexes in vivo, the SAGA, ADA, SALSA, and SLIK complexes (Grant et al., 1997, 1998; Sterner et al., 1999). These interact with transcriptional activators during promoter targeting and with TATA box-binding protein (TBP) during the regulation of basal factor activity (Barlev et al., 1995). The emerging model is that these complexes are recruited to promoters through interactions with sequence-specific activator proteins. GCN5 mediates H3-K9 and H3-K14 acetylation within the basal promoter and subsequently general transcription factors are recruited and transcription is elevated. This general principle is complicated by the fact that multiple modifications occur simultaneously within a single histone tail and on the histone tails contained in a single nucleosome. Coupled with the observation that one histone modification can modulate other modifications, a complex series of events and interactions are proposed to mediate the exact level of transcriptional activity from a single promoter (Kouzarides, 2007).

One such link between these histone modifications is exemplified by MAP kinase-dependent mitogen-stimulated gene expression. This is mediated via H3-S10 phosphorylation and the subsequent recruitment of GCN5 to immediate early gene promoters, such as c-*fos* (Cheung et al., 2000). Consistent with this, the GCN5 HAT domain exhibits ~10-fold higher substrate specificity for an S10-phosphorylated H3 peptide when compared to the corresponding nonphosphorylated control (Cheung et al., 2000). The T11 residue of H3 is also phosphorylated (Preuss et al., 2003). Immunohistochemical analysis revealed H3-T11 phosphorylation to be predominant on mitotic chromosomes and to be enriched at centromeres. Conversely, a structure-function analysis using H3-phosphopeptides and yeast mutants indicated that the T11 residue is essential for GCN5 recruitment and is required for optimal transcription at GCN5-dependent promoters (Clements et al., 2003). Thus, it has been suggested that H3-T11 phosphorylation, in addition to H3-S10 phosphorylation, may play an important role in transcriptional regulation in response to unknown signaling pathways.

In response to DNA damage, DNA structures are rapidly sensed and transduced by either the ATR or ATM phosphatidylinositol 3-kinase-related protein kinases (PIKKs). These phosphorylate a wide variety of substrates including Chk1 and Chk2. While

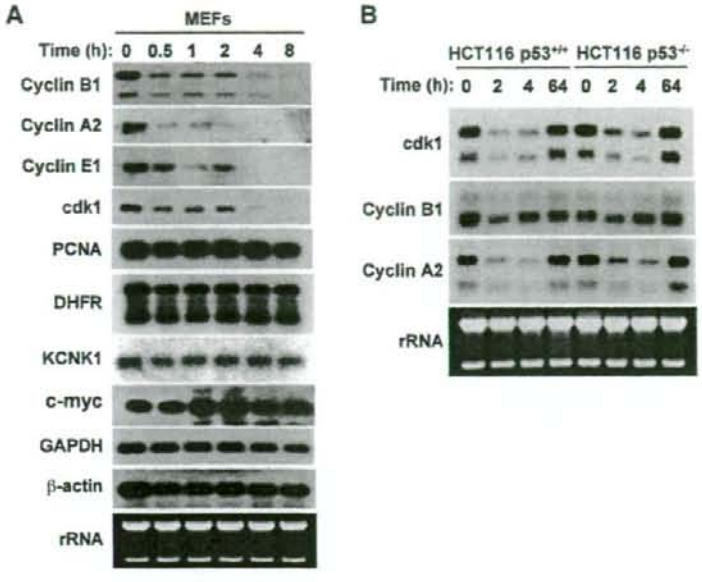

Figure 1. Transcriptional Repression of Cell-Cycle Regulatory Genes following UV Irradiation

(A) Chk1$^{flox/-}$ MEFs were exposed to UV irradiation and harvested at the times indicated. Steady-state transcript levels were detected by northern blotting. 28S and 18S rRNAs are shown stained with ethidium bromide as loading controls. (B) HCT116 p53$^{+/+}$ and HCT116 p53$^{-/-}$ cells were exposed to UV irradiation and transcript levels and rRNAs were detected as in (A).

Chk1 phosphorylation by PIKKs is required for its role in cell-cycle arrest and apoptosis, Chk1 is a constitutively active enzyme and the PIKK-dependent phosphorylation appears not to regulate its kinase activity but rather its subcellular localization. For example, following PIKK-dependent phosphorylation, Chk1 is targeted to centrosomes (Kramer et al., 2004; Niida et al., 2007), where cyclin B1-cdk1 is first activated at the onset of mitosis (Jackman et al., 2003). In undamaged cells, a significant proportion of Chk1 is chromatin associated. Following DNA damage, PIKK-dependent Chk1 phosphorylation results in rapid Chk1 dissociation from chromatin (Smits et al., 2006). Therefore, the possibility exists that chromatin-associated and kinase-active Chk1 mediates unknown functions via phopshorylation of unknown targets.

In this study, we show that DNA damage induces the rapid transcriptional repression of a variety of genes related to cell-cycle progression. This is concomitant with dephosphorylation of H3-T11 and a modest deacetylation of H3-K9. We identify Chk1 as the kinase responsible for H3-T11 phosphorylation and show that Chk1 dissociation from chromatin upon DNA damage closely correlates with decreased H3-T11 phosphorylation. We also demonstrate that, in vitro, GCN5 binds to the H3-pT11 peptide far more efficiently than to unphosphorylated peptide. Taken together, our results suggest a novel mechanism underlying the repression of transcription following DNA damage.

RESULTS

Transcriptional Repression of Cell-Cycle Regulatory Genes in Response to DNA Damage

To investigate the molecular mechanisms underlying the repression of transcription following DNA damage, we used mouse embryonic fibroblasts (MEFs) to examine the steady levels of a variety of cell-cycle regulatory genes after treatment with UV (Figure 1A). Northern blot analysis revealed a decrease in transcript levels for *cyclin B1*, *cyclin A2*, *cyclin E1*, and *cdk1* as early as 0.5 hr after treatment. Levels remained low for the duration of the experiment, being essentially undetectable at the 8 hr time point. These genes are known targets of E2F, raising the possibility that transcriptional repression acts via global effects on E2F activity. To eliminate this possibility, we examined transcript levels of the additional E2F targets, *PCNA*, *DHFR*, and *KCNK1*. *GAPDH* and *β-actin* were used as loading controls. Transcript levels from all five genes remained constant during the course of the experiments. Thus, the repression of transcription of several cell-cycle regulatory genes following DNA damage is independent of both E2F and global effects on transcription. DNA damage-dependent transcriptional repression did not correlate with transcript half life (HL) since c-*myc* transcript (HL 1.2 hr) was constant during the experimental period (*cyclin B1*: HL 2.0 hr, *cdk1*: HL 5.1 hr, *PCNA*: HL 11.7 hr, *KCNK1*: HL 11.7 hr, *GAPDH*: HL 29.5 hr).

p53 is known to function as a negative regulator of *cyclin B1* and *cdk1* transcription (Flatt et al., 2000). We exposed HCT116 p53$^{+/+}$ and an isogenetic derivative, HCT116 p53$^{-/-}$ cells, to UV and examined the levels of *cdk1*, *cyclin B1*, and *cyclin A2* expression (Figure 1B). Expression levels were repressed in a similar manner as previously seen in MEFs and recovered efficiently 64 hr postirradiation. There was no significant difference dependent on the p53 status. Thus, these results indicate that transcriptional repression of a subset of cell-cycle genes is p53 independent.

To establish if changes to the expression of cell-cycle regulatory genes was observed following treatment with other DNA damage agents, we treated MEFs or HCT116 p53$^{+/+}$ cells with either X-ray or bleomycin and examined *cyclin B1* and *cdk1* expression (Figure S1). Both X-ray and bleomycin treatment suppressed *cyclin B1* and *cdk1* expression in a dose- and time-dependent fashion.

Reduction in H3-T11 Phosphorylation after DNA Damage

We examined the known histone H3 modifications (H3-S10 and H3-T11 phosphorylation, H3-AcK9, -AcK14, -AcK18, -AcK23, and H3-MeK79), H2A modification (H2A-AcK5), and H4

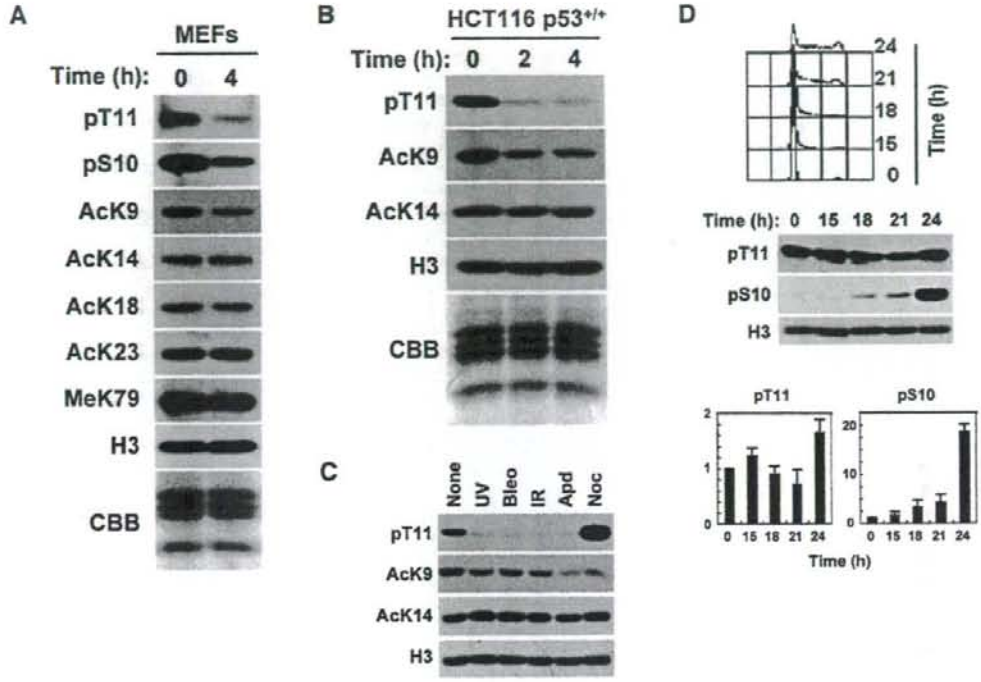

Figure 2. Changes to Core Histone Modifications following DNA Damage

(A) Chk1$^{flox/-}$ MEFs were exposed to UV irradiation. After 4 hr cells were harvested and chromatin fractions prepared and analyzed by immunoblotting for the presence of the indicated histone modifications using modification-specific antibodies. CBB staining of chromatin fractions is shown as a loading control.

(B) HCT116 p53$^{+/+}$ cells were exposed to UV irradiation and analyzed for histone modifications as described for (A).

(C) Chk1$^{flox/-}$ MEF cells were treated with UV, bleomycin (Bleo), X-ray irradiation (IR), aphidicolin (Apd), or nocodazole (Noc). Following exposure (UV: 4 hr, Bleo: 16 hr, IR: 2 hr, Apd: 16 hr, or Noc: 16 hr), changes in histone modifications of the indicated residues were analyzed as in (A). Phosphorylation of H3-T11 and acetylation of H3-K9 were reduced in response to all DNA-damaging agents.

(D) Chk1$^{flox/-}$ MEF cells rendered quiescent by serum starvation (4 days) and growth were restored by the addition of 15% FBS. Cells were harvested at the indicated times and subjected to FACS (top), and chromatin fractions prepared and analyzed by immunoblotting using the indicated antibodies (middle). Changes in H3-T11 or -S10 phosphorylation obtained from three independent experiments are shown as mean ± SD (Bottom). Data were normalized for amount of H3.

modification (H4-AcK8) for global changes. Antibodies specific to the histone modification were used to probe chromatin fractions derived from MEFs either before or 4 hr after UV irradiation (Figure 2A). A significant decrease in both H3-T11 and H3-S10 phosphorylation and a modest decrease in H3-K9 acetylation were observed following DNA damage. In addition, H2A-K5 and H4-K8 acetylations were moderately decreased following DNA damage (data not shown). To establish that this was not a cell line-specific effect, we performed a similar analysis on HCT116 p53$^{+/+}$ cells. We observed similar reductions in H3-T11 phosphorylation plus H3-K9 acetylation (Figure 2B).

To establish if changes to the modifications of histones were observed following treatment with other DNA damage agents, we treated MEFs with either UV, bleomycin, X-rays, or aphidicolin (Figure 2C) and examined levels of H3-T11 phosphorylation and H3-K9 and -K14 acetylation. After verifying the specificity of the anti-phospho-H3-T11 antibody (Figure S2), we observed that each DNA-damaging treatment reduced H3-T11 phosphorylation and H3-K9 acetylation but did not affect H3-K14 acetylation. In contrast, treating cells with nocodazole for 16 hr strongly enhanced H3-T11 phosphorylation but reduced H3-K9 acetylation. This most likely results from an increase in the population of mitotic cells.

Structural analysis revealed that when GCN5 binds to the N-terminal tail of H3, the side chain of H3-T11 is deeply buried in the peptide-binding cleft (Clements et al., 2003). Thus, the increased negative charge associated with H3-T11 phosphorylation may enhance H3-GCN5 interactions. To address this question, we examined the recently solved structure of *Tetrahymena* GCN5 cocrystallized with H3 peptide. By computer modeling, we found that H3-T11 phosphorylation could make substantial van der Waals interactions with the side chains of GCN5-R113, E122, I189, K190, and Y192 without H3-S10 phosphorylation (Figure S3). Thus H3-T11 phosphorylation may have a similar effect on GCN5 interaction as that shown for H3-S10 phosphorylation.

Therefore, we focused our attention on the physiological relevance of H3-T11 phosphorylation during DNA-damage-induced transcriptional repression. It has been reported that H3-T11 phosphorylation is mitosis specific and may facilitate centromere function (Preuss et al., 2003). Mitotic specificity would be inconsistent with our model and therefore we re-examined H3-S10 and H3-T11 phosphorylation during interphase. We synchronized MEFs at quiescence and restarted the cell cycle. H3-S10 phosphorylation was absent in arrested cells and only accumulated later in the time course when FACS profiles suggested that cells were entering mitosis (Figure 2D). In contrast, H3-T11 phosphorylation was readily detectable in extracts from quiescent cells and the level did not vary greatly during the experiment. A maximum (<2-fold increase) was noted at 24 hr. Thus, unlike H3-S10 phosphorylation, H3-T11 phosphorylation is not specific to mitosis. Therefore, the decrease we observed in H3-T11 phosphorylation following DNA damage cannot solely be due to a reduction in the population of mitotic cells.

To further confirm the H3-T11 phosphorylation during interphase, we synchronized HCT116 and Tera-1 cells in quiescence by serum starvation and tsFT210 cells (temperature-sensitive cdk1 mutant) in G2/M phase by culturing at 39°C (Figure S4). Cells were subsequently released into the cell cycle and subjected to FACS analysis and immunoblotting with anti-pT11 antibodies. While H3-T11 phosphorylation was enhanced at mitosis, it was readily detectable during interphase. We conclude that H3-T11 phosphorylation during interphase is not cell type specific.

Chk1 Mediates Phosphorylation of H3-T11 in Interphase

The amino acid sequence surrounding the T11 residue was examined for kinase consensus sequences. A minimum consensus for Chk1-dependent phosphorylation was identified (Figure 3A). Chk1 preferentially phosphorylates its substrates at serine or threonine residues with Lys or Arg located at the −3 position (O'Neill et al., 2002). To establish if Chk1 could phosphorylate H3-T11 in vitro, we performed an in vitro kinase assay using purified H3 or a T11A mutant as substrate. Chk1, but not a kinase-deficient Chk1 (Chk1-K38M), incorporated radiolabeled phosphorous into H3. Substitution of T11 with alanine significantly reduced incorporation, indicating T11 as the main target residue of Chk1 (Figure 3B). Using antibodies specific to H3 phospho-T11, we established that Chk1-phosphorylated H3 contained molecules in which T11 was phosphorylated. H3-pT11 antibodies failed to recognize Chk1-phosphorylated H3-T11A, further confirming its specificity (Figure 3B). In addition to phosphorylating purified H3, we also demonstrated that Chk1 could phosphorylate H3 present either in nucleosomes or mixed with core histones (Figure 3C). This is strong evidence that Chk1 is a physiological histone kinase. We also used a yeast two-hybrid assay (data not shown) to establish that Chk1 could interact with H3. Taken together, our results are consistent with Chk1 being able to phosphorylate H3-T11 in vivo.

To establish if Chk1 is responsible for the in vivo H3-T11 phosphorylation that we have identified in MEFs, $Chk1^{flox/-}$ MEF cells were infected with Cre-adenovirus or LacZ expressing control adenovirus and the status of H3 modifications was examined (Figure 3D). Loss of H3-T11 phosphorylation was modest 1 day after adenovirus infection and pronounced at 2 days. This is consistent with chromatin-bound Chk1 having a half life of 1.2 days (data not shown). A modest reduction in H3-S10 phosphorylation and H3-K9 acetylation was also observed. H3-K14 acetylation was not affected.

Chk1 loss leads to replication fork collapse and subsequent DNA damage during S phase (Syljuasen et al., 2005) and concomitant PIKK activation and Chk2 signaling. Therefore, it remained possible that the decrease in H3-T11 phosphorylation is indirect and caused by responses to the DNA damage induced by Chk1 depletion. To exclude this possibility, we arrested cells by serum starvation before infecting with Ade-Cre virus to eliminate Chk1 in quiescent cells (Figure 3E). Expression of Cre, but not LacZ, in quiescent cells resulted in decreased H3-T11 phosphorylation. The fact that Chk1 depletion did not cause increased single- or double-strand breaks in quiescent cells (Figure S5) strongly indicates that Chk1 is necessary for normal H3-T11 phosphorylation and that loss of Chk1 rapidly results in decreased levels of phosphorylated H3-T11. We also observed that cells synchronized in early S phase by aphidicolin treatment show reduced H3-T11 phosphorylation independent of Chk1 status (Figure 3E). One possible explanation for this is that the aphidicolin-treated cells activate Chk1, mimicking the conditions of DNA damage. Indeed, when Chk1-depleted cells were treated with UV no further reduction in H3-T11 phosphorylation signal was observed (Figure 3F). Our results indicate that Chk1 is required for the in vivo phosphorylation of H3-T11. Interestingly, Chk1 depletion did not result in a pronounced decrease in H3-T11 phosphorylation when MEFs were synchronized by nocodazole treatment (Figure 3E). This is consistent with the existence of a mitotic-specific H3-T11 kinase. Because Chk1 and Chk2 have a similar consensus sequence for phospho-targets, we also examined H3-T11 phosphorylation in $Chk2^{-/-}$ MEFs (Figure 3G). Chk2 was dispensable for in vivo H3-T11 phosphorylation.

Chk1 Chromatin Dissociation after DNA Damage Correlates with H3-T11 Dephosphorylation and Transcript Levels of *cdk1* and *cyclin B1*

Chk1 release from chromatin is triggered by PIKK-dependent phosphorylation and is essential for G2 checkpoint arrest. We observed that Chk1 was largely dissociated from chromatin between 0.5 and 1 hr after DNA damage (Figure 4A). The kinetics of the reduction in H3-T11 phosphorylation were virtually identical. Similarly, the reduction in H3-K9 acetylation followed similar kinetics. H3-K14 acetylation remained unchanged as expected. The decreased phosphorylation of H3-T11 is likely to be due to dephosphorylation because we did not observe release of phosphorylated H3 into the soluble fraction. We next examined UV dose-dependent changes in Chk1 dissociation, γ-H2AX induction, H3-T11 phosphorylation, and *cyclin B1* and *cdk1* expression (Figure S6). A correlation between γ-H2AX induction and Chk1 chromatin dissociation was observed and the kinetics of Chk1 dissociation and the loss of H3-T11 phosphorylation were virtually identical. Importantly, suppression of *cyclin B1* and *cdk1* expression showed similar kinetics.

If Chk1 chromatin dissociation is a causative event for reduced H3-T11 phosphorylation, we would predict that the response should be dependent on the PIKKs. Treatment with caffeine, an